Optimal ultrarobust quantum gates by inverse optimization

Ghassen Dridi [1,2] Xavier Laforgue,[3] Mohamed Mejatty,[2] and Stéphane Guérin [3,*]
[1] *Institut Supérieur des Sciences Appliquées et de Technologies de Gafsa, Université de Gafsa, Campus Universitaire Sidi Ahmed Zarroug, Gafsa 2112, Tunisia*
[2] *Laboratoire de Matériaux Avancés et Phénomènes Quantiques, Faculté des Sciences de Tunis, Université de Tunis El Manar ll, 2092 El Manar Tunis, Tunisia*
[3] *Laboratoire Interdisciplinaire Carnot de Bourgogne, UMR No. 6303, CNRS, Université de Bourgogne, BP 47870, 21078 Dijon, France*

(Received 31 October 2023; revised 23 April 2024; accepted 28 May 2024; published 20 June 2024)

We propose a systematic method to construct robust optimal quantum control at high orders by inverse optimization and apply it for the generation of ultrarobust optimal quantum gates. We derive explicit integrals that characterize robustness up to seventh order against pulse amplitude for time or energy minimization. At fifth order, time optimization is achieved for a flat pulse and a detuning featuring a dual-frequency oscillation. We analyze its performance and compare it to composite pulse techniques: Ultrarobust inverse optimization is considerably faster (in the range 16%–40% depending on the considered gate) than the best composite pulses with similar performance.

DOI: 10.1103/PhysRevA.109.062613

I. INTRODUCTION

Quantum gates are key elements in quantum information and their production, which is resistant against imperfections, is determinant to elaborate practical quantum computers [1]. Well-known alternative methods to standard adiabatic, i.e., slow, approximate, and energetically expensive techniques [2,3] or accelerated adiabatic passage [4–8] use composite techniques [9–16]. Recently, various forms of shortcut to adiabaticity techniques have been proposed, which offer families of exact solutions [17,18]. In particular, protocols based on inverse engineering can achieve robust control via the introduction of arbitrary *Ansätze*, as shown in [19–22]. However, these methods, while exact and potentially faster than standard adiabatic passage, are not specifically designed to be optimal and still cost unnecessary energy and time, which might be detrimental regarding decoherence. In this paper we focus on exact and robust gate achievements adding the requirement of optimality, typically with respect to time or energy. We highlight that we define such an optimality requirement in an absolute way, which is possible when robustness is quantified. More specifically, we apply perturbation theory to determine the transfer profile as a function of the deviation of the ideal controls and a given robustness order that corresponds to the nullification of its derivatives at the corresponding order of perturbation theory.

Optimal control theory (OCT) is a powerful tool to mitigate intensities of the control pulses and speed up the evolution, allowing one in principle to reach the ultimate bounds in the system [23]. Besides numerical implementation of OCT, such as gradient ascent algorithms [24], the Pontryagin maximum principle (PMP) [25–27] allows analytic (or semianalytic) derivation of the optimal controls (typically with respect to time or energy) in a finite-dimensional problem. The PMP using an extended Hilbert space [28] allows an elegant integration of the robustness constraints, but leads to complicated systems to solve.

Two geometric approaches [29–33] have been proposed recently in order to derive optimal and robust solutions operating at the ultimate bounds of the system. One approach, referred to as robust inverse optimization (RIO) [30], is an optimization procedure producing the geodesic minimizing a given cost and constrained by the robustness integrals with boundaries ensuring exact fidelity in the dynamical variable space (typically dynamical angles). The controls are next inversely determined from the time-dependent Schrödinger equation and the derived geodesic. It optimally improves the robust inverse engineering protocols of Refs. [19,20,22] since no *Ansätze* to parametrize the dynamical angles are needed. Analytic solutions can be derived for the problem of robustness with respect to pulse inhomogeneities [33]. The RIO procedure has been demonstrated recently on IBM's quantum computers in a digital version for state-to-state transfer robust against pulse inhomogeneities at third and fifth orders [34].

In this paper the RIO method is reformulated in a systematic way and is referred to as ultra-RIO. We derive in particular the form of the controls robust against pulse inhomogeneities at fifth order for state-to-state transfer (used in [34]) and quantum gates. In this paper we assume a unitary evolution corresponding to gate operations occurring much faster than any decay. Aiming at optimal time is therefore of paramount importance.

The paper is organized as follows. In Sec. II we introduce the model and the inverse-engineering method. In Sec. III we present the single-shot shaped-pulse (SSSP) method, which

*Contact author: sguerin@u-bourgogne.fr

is generalized to solve ultrarobust problems. The method is applied in Sec. IV to derive the differential equations by Euler-Lagrange optimization. Optimal trajectories robust at fifth order against field inhomogeneities are obtained in Sec. V for arbitrary population transfers and in Sec. VI for quantum gates. In Sec. VII we show that the optimal problem robust in the detuning (inhomogeneous broadening) can be treated similarly by RIO. We summarize and discuss our results in Sec. VIII. We present in the Appendixes the details of the calculations.

II. MODEL AND INVERSE-ENGINEERING METHOD

In this section and the next one, we follow the presentation of [33] in order to provide the main elements to be considered for high-order robustness. We study the Hamiltonian

$$H_\lambda = H_0 + \lambda V \tag{1a}$$

$$= \frac{\hbar}{2}\begin{bmatrix} -\Delta & \Omega \\ \Omega & \Delta \end{bmatrix} + \frac{\hbar}{2}\begin{bmatrix} -\delta & \alpha\Omega+\beta \\ \alpha\Omega+\beta & \delta \end{bmatrix}, \tag{1b}$$

where the Hamiltonian

$$H_0 = \frac{\hbar}{2}\begin{bmatrix} -\Delta & \Omega \\ \Omega & \Delta \end{bmatrix} \tag{2}$$

in the basis of $|0\rangle = [1 \quad 0]^T$ and $|1\rangle = [0 \quad 1]^T$ represents the qubit driven by the controls: the pulsed Rabi frequency $\Omega \equiv \Omega(t)$ (considered real without loss of generality) and the detuning $\Delta \equiv \Delta(t)$. The term λV is a perturbation of known form (represented by V) but of unknown amplitude, which is characterized by the parameter $\lambda \equiv (\alpha, \beta, \delta)$. Here α is a coefficient modifying the Rabi field amplitude (pulse inhomogeneities), δ features inhomogeneous broadening or a slow stochastic noise in the energy levels of the qubit (i.e., considered in a quasistatic representation), and β features a slow stochastic transverse noise. Taking the term V as perturbation of the Hamiltonian H_0, we will show that robustness requirements with respect to changes of α, β, and γ can be reduced to a problem of nullifying the derivatives of the excitation profile to a target state order by order (see Sec. III).

The solution of the time-dependent Schrödinger equation (TDSE) $i\hbar\frac{\partial}{\partial t}|\phi_0(t)\rangle = H_0|\phi_0(t)\rangle$ is conveniently parametrized with three angles: the mixing angle $\theta \equiv \theta(t) \in [0, \pi]$, the internal (or relative) phase $\varphi \equiv \varphi(t) \in [-\pi, \pi]$, and a global phase $\gamma \equiv \gamma(t) \in [0, 2\pi]$ as

$$|\phi_0(t)\rangle = \begin{bmatrix} e^{i\varphi/2}\cos(\theta/2) \\ e^{-i\varphi/2}\sin(\theta/2) \end{bmatrix} e^{-i\gamma/2}, \tag{3}$$

corresponding to the equation of motion in the dynamical variable space:

$$\dot\theta = \Omega\sin\varphi, \tag{4a}$$

$$\dot\varphi = \Delta + \Omega\cos\varphi\cot\theta, \tag{4b}$$

$$\dot\gamma = \Omega\frac{\cos\varphi}{\sin\theta} = \dot\theta\frac{\cot\varphi}{\sin\theta}. \tag{4c}$$

The inverse-engineering method consists in determining the Hamiltonian elements from the dynamics by inverting the TDSE $H_0 = i\hbar[\frac{\partial}{\partial t}U_0(t,t_i)]U_0^\dagger(t,t_i)$, i.e., from inversion of Eqs. (4), one can determine the detuning and the Rabi frequency as functions of θ, $\dot\varphi$, and $\dot\gamma$:

$$\Delta = \dot\varphi - \dot\gamma\cos\theta, \tag{5a}$$

$$\Omega = \frac{\dot\theta}{\sin\varphi} = \pm\sqrt{\dot\theta^2 + \dot\gamma^2\sin^2\theta}. \tag{5b}$$

We will consider $\Omega > 0$ without loss of generality for the problem of robustness with respect to pulse inhomogeneities. One can determine from (4c) the phase

$$\varphi = \arctan\left(\frac{\dot\theta}{\dot\gamma\sin\theta}\right), \quad \begin{cases} 0 \leqslant \varphi \leqslant \pi & \text{for } \dot\theta \geqslant 0 \\ -\pi < \varphi < 0 & \text{otherwise.} \end{cases} \tag{6}$$

Equation (4c) links the three angles; we can thus consider two independent dynamical variables. We choose $\theta(t)$ and $\gamma(t)$ for practical technical reasons since the pulse area and energy can be expressed simply as functions of theses angles (shown below) and they provide a geometric representation of the problem. The third dynamical variable $\varphi(t)$ is given by $\cot\varphi = \dot\gamma\sin\theta/\dot\theta$, from which we obtain

$$\dot\varphi = (\ddot\theta\dot\gamma\sin\theta - \ddot\gamma\dot\theta\sin\theta - \dot\gamma\dot\theta^2\cos\theta)/(\dot\theta^2 + \dot\gamma^2\sin^2\theta). \tag{7}$$

One can write the pulse area [defining $\gamma_i \equiv \gamma(t_i)$ and $\gamma_f \equiv \gamma(t_f)$] assuming a monotonic $\gamma(t)$ where the + (−) sign corresponds to $\dot\gamma > 0$ ($\dot\gamma < 0$) as

$$\int_{t_i}^{t_f} dt\,\Omega(t) = \pm\int_{\gamma_i}^{\gamma_f} d\gamma\sqrt{\left(\frac{d\tilde\theta}{d\gamma}\right)^2 + \sin^2\tilde\theta} \equiv \mathcal{A}(\tilde\theta), \tag{8}$$

which does not depend on the time dependence of $\gamma(t)$, but only on $\tilde\theta(\gamma)$ and its derivative. We have defined the dependence on γ as $\tilde\theta(\gamma(t)) \equiv \theta(t)$. In general, when $\gamma(t)$ is not monotonic, we can define piecewise functions $\tilde\theta_j(\gamma)$ in each interval j where $\dot\gamma(t)$ has a constant sign.

The pulse energy in the electric dipole approximation

$$\mathcal{E}(\gamma,\theta) = \int_{t_i}^{t_f} dt\,\Omega^2(t) = \int_{t_i}^{t_f} dt(\dot\theta^2 + \dot\gamma^2\sin^2\theta) \tag{9}$$

depends on the time parametrization of the pulse and thus on the angles $\theta(t)$ and $\gamma(t)$. We will optimize the cost defined as the pulse area $\mathcal{A}$, the pulse energy $\mathcal{E}$ (for a fixed duration $t_f - t_i$), or the duration of the process, i.e., time optimization (for a given peak amplitude of the control). We denote by $|\phi_\lambda(t)\rangle$ the state of the complete dynamics, the solution of the TDSE $i\hbar\frac{\partial}{\partial t}|\phi_\lambda(t)\rangle = H_\lambda|\phi_\lambda(t)\rangle$.

III. GENERAL FORMULATION OF THE SINGLE-SHOT SHAPED-PULSE METHOD FOR THE ULTRAROBUST PROCESS

A. Formulation and figures of merit

From an initial condition at t_i, we assume that the Hamiltonian $H_0(t)$ leads exactly to a given target at the end of the process t_f. The process is robust if a perturbation added to the Hamiltonian leads to a close target at t_f in a way that is defined below.

The SSSP method [20] consists in (i) the perturbative expansion of $|\phi_\lambda(t_f)\rangle$, corresponding typically to a dynamics from the ground state $|\phi_\lambda(t_i)\rangle = |0\rangle$, with respect to λ,

$$\langle\phi_T|\phi_\lambda(t_f)\rangle = 1 + O_1 + O_2 + O_3 + \cdots, \tag{10}$$

where $O_n \equiv O(\lambda^n)$ is defined as the (complex) robustness integral of order n and $|\phi_T\rangle$ the target state, and (ii) the nullification of the coefficients $O_{m\leqslant n}$ to define a robust process at a given order n. It can be formulated in terms of propagators. We define the propagator associated with the unperturbed Hamiltonian $H_0 \equiv H_{0,0,0}$,

$$U_0(t,t_i) = \begin{bmatrix} a \equiv e^{(i/2)(\varphi-\gamma)}\cos(\theta/2) & -\bar{b} \\ b \equiv e^{-(i/2)(\varphi+\gamma)}\sin(\theta/2) & \bar{a}\end{bmatrix}, \tag{11}$$

with $|a|^2 + |b|^2 = 1$ and $U_\lambda(t,t_i)$ associated with the traceless Hamiltonian $H_\lambda(t)$. The perturbative solution reads

$$\begin{aligned} U_\lambda(t_f,t_i) &= U_0(t_f,t_i)\left[\mathbb{1} + \frac{\lambda}{i\hbar}W_1 + \left(\frac{\lambda}{i\hbar}\right)^2 W_2 + \cdots\right] \\ &= U_0(t_f,t_i)\begin{bmatrix} 1 + O_1 + O_2 + \cdots & Q_1 + Q_2 + \cdots \\ -(\bar{Q}_1 + \bar{Q}_2 + \cdots) & 1 + \bar{O}_1 + \bar{O}_2 + \cdots \end{bmatrix}, \end{aligned} \tag{12}$$

with the perturbative matrix terms

$$\lambda^n W_n = \lambda^n \int_{t_i}^{t_f} dt_0 V_I(t_0)\int_{t_i}^{t_0} dt_1 V_I(t_1)\cdots \times \int_{t_i}^{t_{n-2}} dt_{n-1}V_I(t_{n-1}), \tag{13}$$

the perturbation in the interaction representation

$$\lambda V_I(t) = \lambda U_0^\dagger(t,t_i)V(t)U_0(t,t_i) = \hbar\begin{bmatrix} e(t) & f(t) \\ \bar{f}(t) & -e(t)\end{bmatrix}, \tag{14}$$

the matrix elements

$$O_n = \left(\frac{\lambda}{i\hbar}\right)^n \langle 0|W_n|0\rangle, \quad Q_n = \left(\frac{\lambda}{i\hbar}\right)^n \langle 1|W_n|0\rangle, \tag{15}$$

and the functions

$$e(t) = \frac{1}{2}[-\delta\cos\theta + (\alpha\Omega + \beta)\cos\varphi\sin\theta] \equiv \sum_{\lambda=\alpha,\beta,\delta}\lambda e_\lambda, \tag{16a}$$

$$f(t) = \frac{1}{2}[\delta\sin\theta + \alpha(\dot{\gamma}\sin\theta\cos\theta - i\dot{\theta}) + \beta(\cos\varphi\cos\theta - i\sin\varphi)]e^{i\gamma} \equiv \sum_{\lambda=\alpha,\beta,\delta}\lambda f_\lambda. \tag{16b}$$

The unitarity of the solution (12) imposes

$$|1 + O_1 + O_2 + \cdots|^2 + |Q_1 + Q_2 + \cdots|^2 = 1. \tag{17}$$

1. Population transfer

For the case of a population transfer to a target state $|\phi_T\rangle$ (of given angle θ_0 and internal phase φ_0), the final global phase γ_f is irrelevant and one can consider the figure of merit

$$\mathcal{F}_{\rm pt} = |\langle\phi_T|\phi_\lambda(t_f)\rangle|^2 = 1 + \tilde{O}_1 + \tilde{O}_2 + \tilde{O}_3 + \cdots, \tag{18}$$

i.e., up to order n,

$$\mathcal{F}_{\rm pt}^{(n)} = 1 + \sum_{m=1}^{n}\tilde{O}_m, \tag{19}$$

where $\tilde{O}_n$ denotes the term of order n related to the O_n as

$$\tilde{O}_{2n} = |O_n|^2 + 2\sum_{m=0}^{n-1}\mathrm{Re}(O_{2n-m}\bar{O}_m), \tag{20a}$$

$$\tilde{O}_{2n+1} = 2\sum_{m=0}^{n}\mathrm{Re}(O_{2n+1-m}\bar{O}_m), \tag{20b}$$

with $O_0 = 1$. This gives, for the first terms,

$$\tilde{O}_1 = 2\,\mathrm{Re}(O_1) = 0, \tag{21a}$$
$$\tilde{O}_2 = |O_1|^2 + 2\,\mathrm{Re}(O_2), \tag{21b}$$
$$\tilde{O}_3 = 2[\mathrm{Re}(O_3) + \mathrm{Re}(O_2\bar{O}_1)], \tag{21c}$$
$$\tilde{O}_4 = |O_2|^2 + 2[\mathrm{Re}(O_4) + \mathrm{Re}(O_3\bar{O}_1)]. \tag{21d}$$

Inserting the fidelity (18) into the unitarity condition (17) leads to

$$\tilde{O}_1 + \tilde{O}_2 + \tilde{O}_3 + \cdots = -|Q_1 + Q_2 + \cdots|^2, \tag{22}$$

which allows one to identify order by order the corrections to the population transfer as functions of the off-diagonal terms of the perturbative matrix of (12):

$$\begin{aligned}\tilde{O}_{2n+1} &= -2\sum_{m=1}^{n}\mathrm{Re}(Q_{2n+1-m}\bar{Q}_m) \\ &= 0 \quad \text{when } \tilde{O}_{2(m\leqslant n)} = 0,\end{aligned} \tag{23a}$$

$$\begin{aligned}\tilde{O}_{2n} &= -|Q_n|^2 - 2\sum_{m=1}^{n-1}\mathrm{Re}(Q_{2n-m}\bar{Q}_m) \\ &= -|Q_n|^2 \quad \text{when } \tilde{O}_{2(m<n)} = 0.\end{aligned} \tag{23b}$$

This in general gives expressions simpler than (but equivalent to) (21); the first terms read

$$\tilde{O}_1 = 0, \tag{24a}$$
$$\tilde{O}_2 = -|Q_1|^2, \tag{24b}$$
$$\tilde{O}_3 = 0 \quad \text{when } \tilde{O}_2 = 0, \tag{24c}$$
$$\tilde{O}_4 = -|Q_2|^2 \quad \text{when } \tilde{O}_2 = 0, \tag{24d}$$
$$\tilde{O}_5 = 0 \quad \text{when } \tilde{O}_2 = \tilde{O}_4 = 0, \tag{24e}$$
$$\tilde{O}_6 = -|Q_3|^2 \quad \text{when } \tilde{O}_2 = \tilde{O}_4 = 0, \tag{24f}$$
$$\tilde{O}_7 = 0 \quad \text{when } \tilde{O}_2 = \tilde{O}_4 = \tilde{O}_6 = 0. \tag{24g}$$

It shows that the cancellation up to an even order $2n$, $\tilde{O}_{2(m\leqslant n)} = 0$, is obtained for $Q_{m\leqslant n} = 0$, which implies that the next term automatically cancels out, $\tilde{O}_{2n+1} = 0$, i.e., for a given n and for all $m \leqslant n$:

$$\tilde{O}_{2(m\leqslant n)} = \tilde{O}_{2(m\leqslant n)+1} = 0 \quad \text{when } Q_{m\leqslant n} = 0. \tag{25}$$

We conclude that the cancellation of the error up to an order $2n+1$ is satisfied, i.e., $\mathcal{F}_{\rm pt}^{(2n+1)} = 1$, when $Q_{m\leqslant n} = 0$.

2. Quantum gate: Trace fidelity

A figure of merit often adopted to determine the fidelity of a quantum gate is defined as the trace fidelity

$$\mathcal{F}_{\mathrm{g,t}} = \tfrac{1}{2}|\mathrm{Tr}(U_0^\dagger U)| = \mathrm{Re}\langle\phi_T(t_f)|\phi_\lambda(t_f)\rangle, \tag{26}$$

i.e., up to order $2n+1$:

$$\mathcal{F}_{\mathrm{g,t}}^{(n)} = 1 + \sum_{m=1}^{2n+1} \mathrm{Re}(O_m). \tag{27}$$

It can be determined by combining (20) and (23):

$$\begin{aligned}\mathrm{Re}(O_{2n+1}) &= -\sum_{m=1}^{n}[\mathrm{Re}(O_{2n+1-m}\bar{O}_m) + \mathrm{Re}(Q_{2n+1-m}\bar{Q}_m)]\\ &= 0 \quad \text{when } \mathrm{Re}(O_{2n}) = 0, \end{aligned}\tag{28a}$$

$$\begin{aligned}\mathrm{Re}(O_{2n}) &= -\frac{1}{2}(|O_n|^2 + |Q_n|^2)\\ &\quad - \sum_{m=1}^{n-1}[\mathrm{Re}(O_{2n-m}\bar{O}_m) + \mathrm{Re}(Q_{2n-m}\bar{Q}_m)]\\ &= -\frac{1}{2}(|O_n|^2 + |Q_n|^2) \quad \text{when } \mathrm{Re}(O_{2(m<n)}) = 0. \end{aligned}\tag{28b}$$

The first terms read

$$\mathrm{Re}(O_1) = 0, \tag{29a}$$

$$\mathrm{Re}(O_2) = -\tfrac{1}{2}(|O_1|^2 + |Q_1|^2), \tag{29b}$$

$$\mathrm{Re}(O_3) = 0 \quad \text{when } \mathrm{Re}(O_2) = 0, \tag{29c}$$

$$\mathrm{Re}(O_4) = -\tfrac{1}{2}(|O_2|^2 + |Q_2|^2) \quad \text{when } \mathrm{Re}(O_2) = 0, \tag{29d}$$

$$\mathrm{Re}(O_5) = 0 \quad \text{when } \mathrm{Re}(O_2) = \mathrm{Re}(O_4) = 0, \tag{29e}$$

$$\mathrm{Re}(O_6) = -\tfrac{1}{2}(|O_3|^2 + |Q_3|^2) \quad \text{when } \mathrm{Re}(O_2) = \mathrm{Re}(O_4) = 0. \tag{29f}$$

It shows that the cancellation up to an even order $2n$, $\mathrm{Re}(O_{2(m\leqslant n)}) = 0$, is obtained for $O_{m\leqslant n} = 0$ and $Q_{m\leqslant n} = 0$, which implies that the next term automatically cancels out, $\mathrm{Re}(O_{2n+1}) = 0$, i.e., for a given n and for all $m \leqslant n$:

$$\begin{aligned}&\mathrm{Re}(O_{2(m\leqslant n)}) = \mathrm{Re}(O_{2(m\leqslant n)+1}) = 0\\ &\text{when } O_{m\leqslant n} = Q_{m\leqslant n} = 0.\end{aligned}\tag{30}$$

We conclude that the cancellation of the error up to an order $2n+1$ is satisfied, i.e., $\mathcal{F}_{\mathrm{g,t}}^{(2n+1)} = 1$, when $O_{m\leqslant n} = Q_{m\leqslant n} = 0$.

3. Connection between trace and Frobenius fidelities

A more accurate fidelity can be used if one considers all the elements of the gate (12), i.e., both O_m and Q_m at an order m. This corresponds to the Frobenius distance fidelity (or Frobenius fidelity for short) that can be considered up to an order n:

$$\mathcal{F}_{\mathrm{g,d}}^{(n)} = 1 - \sum_{m=1}^{n}\sqrt{|O_m|^2 + |Q_m|^2} \tag{31a}$$

$$= 1 - \sum_{m=1}^{n}\sqrt{-2\,\mathrm{Re}(O_{2m})}. \tag{31b}$$

One concludes that the correction of the Frobenius fidelity at order n is zero, i.e., $\mathcal{F}_{\mathrm{g,d}}^{(n)} = 1$, when the corrections of the trace fidelity up to order $2n$ are zero, $\mathrm{Re}(O_{2(m\leqslant n)}) = 0$, i.e., $O_{m\leqslant n} = Q_{m\leqslant n} = 0$, i.e., $\mathcal{F}_{\mathrm{g,t}}^{(2n+1)} = 1$.

We mostly use the trace fidelity convention in the paper. The corresponding Frobenius fidelity can be deduced from the above arguments. For instance, to a trace fidelity up to order 5 corresponds a Frobenius distance fidelity up to order 2.

B. Integrals of robustness

In Appendix A we determine the first integrals of robustness, $|Q_n|$ (A4) for the population transfer, complemented by the $|O_n|$ (A7) for the quantum gate. The results are summarized in Table I for the first terms.

C. Integrals for population transfer

The fourth (and consequently the fifth) order is zero, $\tilde{O}_4 = 0$, when (i) $\int_{t_i}^{t_f} dt\, f(t) = 0$ and (ii)

$$\int_{t_i}^{t_f} e(t)\int_{t_i}^{t} f(t')dt'dt = 0, \tag{32}$$

i.e.,

$$\int_{t_i}^{t_f} e(t)x(t)dt = 0, \qquad \int_{t_i}^{t_f} e(t)y(t)dt = 0, \tag{33}$$

where we have introduced the new dynamical variables which augment the dimension of the problem,

$$x(t) := \int_{t_i}^{t} a(t')dt', \quad \dot{x}(t) = a(t), \tag{34a}$$

$$y(t) := \int_{t_i}^{t} b(t')dt', \quad \dot{y}(t) = b(t), \tag{34b}$$

with $x(t_i) = 0$ and $y(t_i) = 0$, where we have defined

$$a(t) = \mathrm{Re}[f(t)], \quad b(t) = \mathrm{Im}[f(t)], \tag{35}$$

i.e.,

$$\begin{aligned}2a &= (\delta\sin\theta + \alpha\dot{\gamma}\sin\theta\cos\theta + \beta\cos\varphi\cos\theta)\cos\gamma\\ &\quad + (\alpha\dot{\theta} + \beta\sin\varphi)\sin\gamma,\end{aligned}\tag{36a}$$

$$\begin{aligned}2b &= (\delta\sin\theta + \alpha\dot{\gamma}\sin\theta\cos\theta + \beta\cos\varphi\cos\theta)\sin\gamma\\ &\quad - (\alpha\dot{\theta} + \beta\sin\varphi)\cos\gamma.\end{aligned}\tag{36b}$$

The α robustness, involving the functions from (16)

$$e/\alpha = \tfrac{1}{2}\dot{\gamma}\sin^2\theta \equiv e_\alpha, \tag{37a}$$

$$f/\alpha = \tfrac{1}{2}(\dot{\gamma}\sin\theta\cos\theta - i\dot{\theta}) \equiv f_\alpha \tag{37b}$$

and

$$x_\alpha(t) := \int_{t_i}^{t} a_\alpha(t')dt', \quad \dot{x}_\alpha(t) = a_\alpha(t), \tag{38a}$$

$$y_\alpha(t) := \int_{t_i}^{t} b_\alpha(t')dt', \quad \dot{y}_\alpha(t) = b_\alpha(t), \tag{38b}$$

with

$$a_\alpha \equiv a/\alpha = \tfrac{1}{2}\dot{\gamma}\sin\theta\cos\theta\cos\gamma + \tfrac{1}{2}\dot{\theta}\sin\gamma, \tag{39a}$$

$$b_\alpha \equiv b/\alpha = \tfrac{1}{2}\dot{\gamma}\sin\theta\cos\theta\sin\gamma - \tfrac{1}{2}\dot{\theta}\cos\gamma, \tag{39b}$$

TABLE I. Conditions for robustness at order $2n+1$ (with the trace fidelity convention for the quantum gate). Population transfer robustness requires the (cumulated) conditions in column 2, while gate robustness requires both columns 2 and 3.

$2n+1$	$\tilde{O}_n = 0 \cup$	$\mathrm{Re}(O_m) = 0 \cup$
3	$\int_{t_i}^{t_f} f(t)dt = 0$	$\int_{t_i}^{t_f} e(t)dt = 0$
5	$\int_{t_i}^{t_f} e(t) \int_{t_i}^{t} f(t')dt'dt = 0$	$\int_{t_i}^{t_f} f(t) \int_{t_i}^{t} \bar{f}(t')dt'dt = 0$
7	$\int_{t_i}^{t_f} \{f(t)[\int_{t_i}^{t} e(t')dt']^2 + \bar{f}(t)\lvert \int_{t_i}^{t} f(t')dt'\rvert^2\}dt = 0$	$\int_{t_i}^{t_f} e(t)\lvert \int_{t_i}^{t} f(t')dt'\rvert^2 dt = 0$

is thus satisfied at fifth order for (i) $\int_{t_i}^{t_f} f_\alpha(t)dt = 0$ and (ii) Eq. (32):

$$\int_{t_i}^{t_f} dt\, \dot{\gamma} x_\alpha \sin^2\theta = 0, \quad \int_{t_i}^{t_f} dt\, \dot{\gamma} y_\alpha \sin^2\theta = 0. \tag{40}$$

Cancellation of the sixth (and consequently the seventh) order, $\tilde{O}_6 = 0$, requires in addition

$$\int_{t_i}^{t_f} \{f(t)z^2(t) + \bar{f}(t)[a^2(t) + b^2(t)]\}dt = 0 \tag{41}$$

with the dynamical variable

$$z(t) = \int_{t_i}^{t} e(t')dt', \quad \dot{z}(t) = e(t). \tag{42}$$

D. Integrals for the quantum gate

The fourth order involves in addition

$$\mathrm{Im} \int_{t_i}^{t_f} f(t)dt \int_{t_i}^{t} \bar{f}(t')dt' = \int_{t_i}^{t_f} dt \int_{t_i}^{t} [a(t')b(t) - a(t)b(t')]dt'. \tag{43}$$

According to Table I, the α robustness at fourth order (and thus at fifth order) requires (i)

$$\int_{t_i}^{t_f} e(t)dt = 0, \tag{44a}$$

(ii) $\int_{t_i}^{t_f} f(t)dt = 0$ and $\int_{t_i}^{t_f} f(t) \int_{t_i}^{t} \bar{f}(t')dt'dt = 0$, which both can be satisfied via (A7c) for

$$\left| \int_{t_i}^{t_f} f(t)dt \right|^2 = \frac{1}{2}\int_{t_i}^{t_f} dt\, \dot{\gamma} \sin 2\theta (x_\alpha \cos\gamma + y_\alpha \sin\gamma) + \int_{t_i}^{t_f} dt\, \dot{\theta}(x_\alpha \sin\gamma - y_\alpha \cos\gamma) = 0, \tag{44b}$$

$$\frac{2}{\alpha^2}\mathrm{Im}\left(\int_{t_i}^{t_f} f(t)dt \int_{t_i}^{t} \bar{f}(t')dt' \right) = \frac{1}{2}\int_{t_i}^{t_f} dt\, \dot{\gamma} \sin 2\theta (x_\alpha \sin\gamma - y_\alpha \cos\gamma) - \int_{t_i}^{t_f} dt\, \dot{\theta}(x_\alpha \cos\gamma + y_\alpha \sin\gamma) = 0, \tag{44c}$$

respectively, and (iii) Eq. (40).

Cancellation of $\mathrm{Re}(O_6)$ [and thus $\mathrm{Re}(O_7)$] requires in addition

$$\int_{t_i}^{t_f} dt\, e(t) \left| \int_{t_i}^{t} dt' f(t') \right|^2 = 0. \tag{45}$$

IV. OPTIMAL α-ROBUST CONTROL: ARBITRARY QUANTUM GATE

In this section we treat explicitly the problem of the α-robust optimal quantum gate (i.e., robust against pulse inhomogeneities) and derive the corresponding differential equations by Euler-Lagrange optimization that optimally satisfy the cancellation of the integrals of columns 2 and 3 of Table I at fifth order. The solutions in terms of the control parameters (detuning and field amplitude) are next determined numerically. The problem of population transfer is treated in the next section as a particular case (where the integrals of column 2 of Table I are considered). The quantum gates are derived in Sec. VI.

An arbitrary SU(2) gate corresponds to

$$U(\theta_0, \varphi_0, \gamma_0) = \begin{bmatrix} c \equiv e^{(i/2)(\varphi_0 - \gamma_0)} \cos(\theta_0/2) & -\bar{d} \\ d \equiv e^{-(i/2)(\varphi_0 + \gamma_0)} \sin(\theta_0/2) & \bar{c} \end{bmatrix}, \tag{46}$$

with the angle θ_0 and the two phases φ_0 and γ_0 to be controlled in a robust way. We can consider without loss of generality the construction of a robust process driving the initial ground state $|0\rangle$ to the state

$$|\phi(t_f)\rangle = |\phi_T\rangle \equiv \begin{bmatrix} e^{i\varphi_0/2} \cos(\theta_0/2) \\ e^{-i\varphi_0/2} \sin(\theta_0/2) \end{bmatrix} e^{-i\gamma_0/2}, \tag{47}$$

where the two final phases $\varphi_f = \varphi_0$ and $\gamma_f = \gamma_0$, while of robust values, are not fixed *a priori*; they result from the optimization procedure.

We highlight that application of a preliminary phase gate (of phase κ)

$$\Phi_\kappa = \begin{bmatrix} e^{-i\kappa/2} & 0 \\ 0 & e^{i\kappa/2} \end{bmatrix} \tag{48}$$

allows one to modify the global phase γ_0: $\gamma_0 \to \gamma_0 + \kappa$. The phase gate can be generated by applying two successive optimal robust NOT gates [33]. On the other hand, adding a static phase η_0 to the control field Ω allows the modification of the internal phase φ_0 of the state: $\Omega \to \Omega e^{-i\eta_0}$ gives $\varphi_0 \to \varphi_0 - \eta_0$.

Equation (4c) implies $\varphi_i = \pi/2$. The problem features thus the boundaries

$$\theta_i = 0, \quad \theta_f = \theta_0, \quad \gamma_i = \varphi_i = \pi/2. \tag{49}$$

The fidelity is given by (27). The equations corresponding to the optimal quantum gate trajectory $\tilde{\theta}(\gamma)$ with respect to pulse area at fifth order are determined in Appendix B.

A. Optimization with respect to energy or time at fifth order

Robustness at fifth order corresponds to the five constraints (44) that lead to the five integrals in the formalism of Euler-Lagrange optimization

$$\psi_0(\gamma,\theta) \equiv \int_{t_i}^{t_f} dt\, \dot{\gamma}\sin^2\theta \equiv \int_{t_i}^{t_f} dt\, \varphi_0(\dot{\gamma},\theta) = 0, \tag{50a}$$

$$\begin{aligned}\psi_1(\gamma,\theta,x_\alpha,y_\alpha) &= \frac{1}{2}\int_{t_i}^{t_f} dt\, \dot{\gamma}\sin 2\theta(x_\alpha\cos\gamma + y_\alpha\sin\gamma)\\ &\quad + \int_{t_i}^{t_f} dt\, \dot{\theta}(x_\alpha\sin\gamma - y_\alpha\cos\gamma)\\ &\equiv \int_{t_i}^{t_f} dt\, \varphi_1(\gamma,\dot{\gamma},\theta,\dot{\theta},x_\alpha,y_\alpha) = 0,\end{aligned} \tag{50b}$$

$$\begin{aligned}\psi_2(\gamma,\theta,x_\alpha,y_\alpha) &= \frac{1}{2}\int_{t_i}^{t_f} dt\, \dot{\gamma}\sin 2\theta(y_\alpha\cos\gamma - x_\alpha\sin\gamma)\\ &\quad + \int_{t_i}^{t_f} dt\, \dot{\theta}(x_\alpha\cos\gamma + y_\alpha\sin\gamma)\end{aligned} \tag{50c}$$

$$\equiv \int_{t_i}^{t_f} dt\, \varphi_2(\gamma,\dot{\gamma},\theta,\dot{\theta},x_\alpha,y_\alpha) = 0, \tag{50d}$$

$$\begin{aligned}\psi_3(\gamma,\theta,x_\alpha) &= \int_{t_i}^{t_f} dt\, \dot{\gamma}x_\alpha\sin^2\theta\\ &\equiv \int_{t_i}^{t_f} dt\, \varphi_3(\dot{\gamma},\theta,x_\alpha) = 0,\end{aligned} \tag{50e}$$

$$\begin{aligned}\psi_4(\gamma,\theta,y_\alpha) &= \int_{t_i}^{t_f} dt\, \dot{\gamma}y_\alpha\sin^2\theta\\ &\equiv \int_{t_i}^{t_f} dt\, \varphi_4(\dot{\gamma},\theta,y_\alpha) = 0,\end{aligned} \tag{50f}$$

complemented by the equations (38) governing the variables x_α and y_α, which augment the dimension of the problem,

$$\dot{x}_\alpha = \tfrac{1}{4}\dot{\gamma}\sin 2\theta\cos\gamma + \tfrac{1}{2}\dot{\theta}\sin\gamma \equiv u(\gamma,\dot{\gamma},\theta,\dot{\theta}), \tag{51a}$$

$$\dot{y}_\alpha = \tfrac{1}{4}\dot{\gamma}\sin 2\theta\sin\gamma - \tfrac{1}{2}\dot{\theta}\cos\gamma \equiv v(\gamma,\dot{\gamma},\theta,\dot{\theta}), \tag{51b}$$

with the boundaries [from the constraint $\int_{t_i}^{t_f} f(t)dt = 0$ at the final time]

$$x_\alpha(t_i) = x_\alpha(t_f) = 0, \quad y_\alpha(t_i) = y_\alpha(t_f) = 0. \tag{52}$$

The trajectories $\gamma(t)$, $\theta(t)$, $x_\alpha(t)$, and $y_\alpha(t)$ are a solution of the Euler-Lagrange equations

$$\frac{\partial\mathcal{L}}{\partial\gamma} - \frac{d}{dt}\left(\frac{\partial\mathcal{L}}{\partial\dot{\gamma}}\right) = 0, \tag{53a}$$

$$\frac{\partial\mathcal{L}}{\partial\theta} - \frac{d}{dt}\left(\frac{\partial\mathcal{L}}{\partial\dot{\theta}}\right) = 0, \tag{53b}$$

$$\frac{\partial\mathcal{L}}{\partial x_\alpha} - \frac{d}{dt}\left(\frac{\partial\mathcal{L}}{\partial\dot{x}_\alpha}\right) = 0, \tag{53c}$$

$$\frac{\partial\mathcal{L}}{\partial y_\alpha} - \frac{d}{dt}\left(\frac{\partial\mathcal{L}}{\partial\dot{y}_\alpha}\right) = 0, \tag{53d}$$

with

$$\begin{aligned}\mathcal{L} &= \mathcal{L}_0(\dot{\gamma},\theta,\dot{\theta}) + \lambda_0\varphi_0(\dot{\gamma},\theta) + \sum_{j=1}^{4}\lambda_j\varphi_j\\ &\quad + \mu_x(t)[\dot{x}_\alpha - u(\gamma,\dot{\gamma},\theta,\dot{\theta})]\\ &\quad + \mu_y(t)[\dot{y}_\alpha - v(\gamma,\dot{\gamma},\theta,\dot{\theta})].\end{aligned} \tag{54}$$

In Appendix C we show that they form a system of six differential equations

$$\begin{aligned}&\ddot{\gamma} + 2\dot{\gamma}\dot{\theta}\cot\theta + (\lambda_0 - \lambda_2/2)\dot{\theta}\cot\theta\\ &\quad + \dot{\theta}(\kappa_x\cos\gamma + \kappa_y\sin\gamma) + \lambda_2\dot{\theta}(x_\alpha\sin\gamma - y_\alpha\cos\gamma)\\ &\quad + (\lambda_3x_\alpha + \lambda_4y_\alpha)\dot{\theta}\cot\theta = 0,\end{aligned} \tag{55a}$$

$$\begin{aligned}&\dot{\gamma}^2\sin\theta\cos\theta - \ddot{\theta} + (\lambda_0 - \lambda_2/2)\dot{\gamma}\sin\theta\cos\theta\\ &\quad + [\lambda_2(x_\alpha\sin\gamma - y_\alpha\cos\gamma) + \kappa_x\cos\gamma + \kappa_y\sin\gamma]\dot{\gamma}\sin^2\theta\\ &\quad + (\lambda_3x_\alpha + \lambda_4y_\alpha)\dot{\gamma}\sin\theta\cos\theta = 0,\end{aligned} \tag{55b}$$

$$\dot{\kappa}_x = \lambda_3\dot{\gamma}\sin^2\theta, \tag{55c}$$

$$\dot{\kappa}_y = \lambda_4\dot{\gamma}\sin^2\theta, \tag{55d}$$

$$\dot{x}_\alpha = \dot{\gamma}\sin\theta\cos\theta\cos\gamma + \dot{\theta}\sin\gamma, \tag{55e}$$

$$\dot{y}_\alpha = \dot{\gamma}\sin\theta\cos\theta\sin\gamma - \dot{\theta}\cos\gamma, \tag{55f}$$

with the six Lagrangian multipliers λ_0, λ_2, λ_3, λ_4, $\kappa_{x,i} \equiv \kappa_x(t_i)$, and $\kappa_{y,i} \equiv \kappa_y(t_i)$ (where we have redefined $\kappa_x \to 2\kappa_x$, $\kappa_y \to 2\kappa_y$, $\lambda_3 \to 2\lambda_3$, $\lambda_4 \to 2\lambda_4$, $x_\alpha \to x_\alpha/2$, and $y_\alpha \to y_\alpha/2$), which define the optimal robust trajectory. Concerning the constraints, we have the five integrals (50) and the final boundary (52) on x_α and y_α that can be gathered as a single integral

$$x_\alpha^2(t_f) + y_\alpha^2(t_f) = 0, \tag{56}$$

which coincides with (44b).

We have, as in the lower-order case, the constant of motion given by

$$0 = \frac{d}{dt}(\dot{\theta}^2 + \dot{\gamma}^2\sin^2\theta), \tag{57}$$

which leads to a constant pulse Ω_0:

$$\dot{\theta}^2 + \dot{\gamma}^2\sin^2\theta = \Omega_0^2. \tag{58}$$

If we assume at initial time that $|\dot{\gamma}_i| < \infty$, we conclude that

$$|\dot{\theta}_i| = |\Omega_0|. \tag{59}$$

From (55a) at the initial time

$$2\dot{\gamma}_i\dot{\theta}_i + (\lambda_0 - \lambda_2/2)\dot{\theta}_i = 0, \tag{60}$$

we conclude that

$$\dot{\gamma}_i = -\lambda_0/2 + \lambda_2/4. \tag{61}$$

We show in Appendix D that we recover the optimal trajectory with respect to pulse area from the optimal trajectory with respect to energy, defined by Eqs. (55).

We conclude that the problem of minimizing the pulse area $\mathcal{A}$ (8) is equivalent to minimizing the time under the constraint on the bounded control $\Omega \leqslant \Omega_0$, and the minimum time

$$T_{\min} \equiv (t_f - t_i)_{\min} = \frac{1}{\Omega_0}\int_{\gamma_i}^{\gamma_f} d\gamma \sqrt{(\dot{\tilde{\theta}})^2 + \sin^2\theta} \tag{62}$$

is achieved when the pulse reaches its maximum at all times $\Omega = \Omega_0$. The optimization with respect to the pulse energy (78) uses the same formula (and the same trajectory), but interpreted differently: The minimum (constant) pulse amplitude $\Omega_{0,\min}$ is determined from a given duration $T \equiv t_f - t_i$ of the interaction as

$$\Omega_{0,\min} = \frac{1}{T}\int_{\gamma_i}^{\gamma_f} d\gamma \sqrt{(\dot{\tilde{\theta}})^2 + \sin^2\theta}. \tag{63}$$

B. Expression of detuning

One can express the detuning as a function of the angles θ and γ as follows. Deriving (4c) as

$$\dot{\gamma}\sin\theta = \Omega_0\cos\varphi \tag{64}$$

leads to

$$\ddot{\gamma}\sin\theta + \dot{\gamma}\dot{\theta}\cos\theta = -\dot{\varphi}\Omega_0\sin\varphi = -\dot{\varphi}\dot{\theta}, \tag{65}$$

which allows the substitution of $\dot{\varphi}$ (4b) in

$$\Delta = \dot{\varphi} - \dot{\gamma}\cos\theta \tag{66}$$

to give

$$\Delta = -\frac{1}{\dot{\theta}}(\ddot{\gamma}\sin\theta + 2\dot{\gamma}\dot{\theta}\cos\theta). \tag{67}$$

Using (55a), we finally obtain

$$\Delta = (\lambda_0 - \lambda_2/2 + \lambda_3 x_\alpha + \lambda_4 y_\alpha)\cos\theta + [\kappa_x\cos\gamma + \kappa_y\sin\gamma + \lambda_2(x_\alpha\sin\gamma - y_\alpha\cos\gamma)]\sin\theta. \tag{68}$$

This gives, in particular, at initial time,

$$\Delta_i = \lambda_0 - \lambda_2/2. \tag{69}$$

One can remark that the above formulation can be reduced to the case of (arbitrary) population transfer by taking $\lambda_0 = \lambda_2 = 0$, as studied below.

V. OPTIMAL α-ROBUST COMPLETE POPULATION TRANSFER: NUMERICAL RESULTS

Optimal α-robust population transfer with respect to energy or time at fifth order is given by the trajectory solution of Eqs. (55) with the boundaries (49), but with $\lambda_0 = \lambda_2 = 0$ since both (44a) and (44c) do not hold. We notice that Eq. (4c) also imposes $\varphi_f = \pi/2$ only in the case of complete population transfer. The problem is investigated in detail in Appendix E 1 for the case of complete population transfer (i.e., with $\theta_0 = \pi$). We assume a symmetric trajectory (E5), i.e., with conditions (E8) and (E10). We determine numerically λ_3=1.110 84, λ_4= − 0.849 18, $\kappa_{x,i} = -0.456\,33$, $\kappa_{y,i} = -0.722\,26$, $\gamma_f = 1.0845\pi$, and the minimum time

$$T_{\min} = 2.7102\pi/\Omega_0. \tag{70}$$

The resulting trajectory, detuning, dynamics, and robustness profile are shown in Figs. 1–4, respectively. We notice the

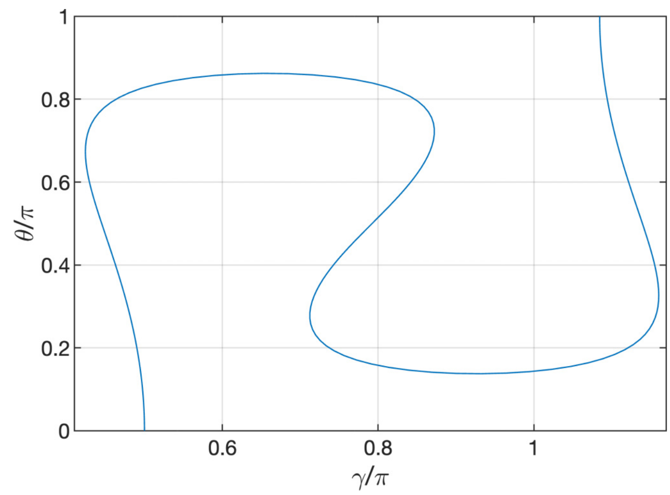

FIG. 1. Optimal robust geodesic $\tilde{\theta}(\gamma)$ corresponding to the optimal fifth-order robust complete population transfer.

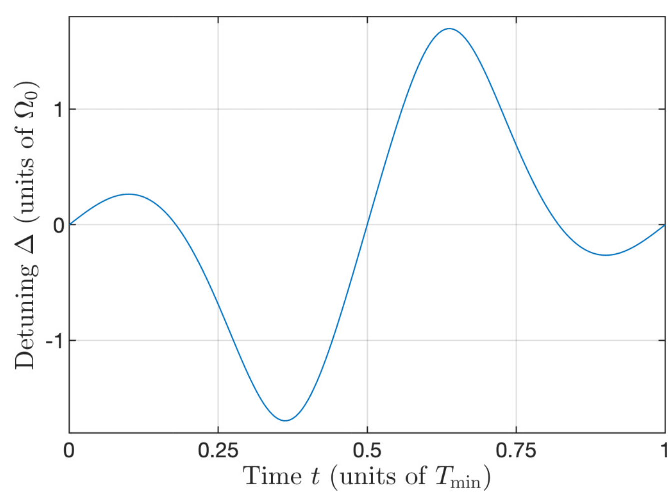

FIG. 2. Detuning (68) corresponding to the time-optimal fifth-order robust complete population transfer, of trajectory shown in Fig. 1 with a constant Rabi coupling Ω_0.

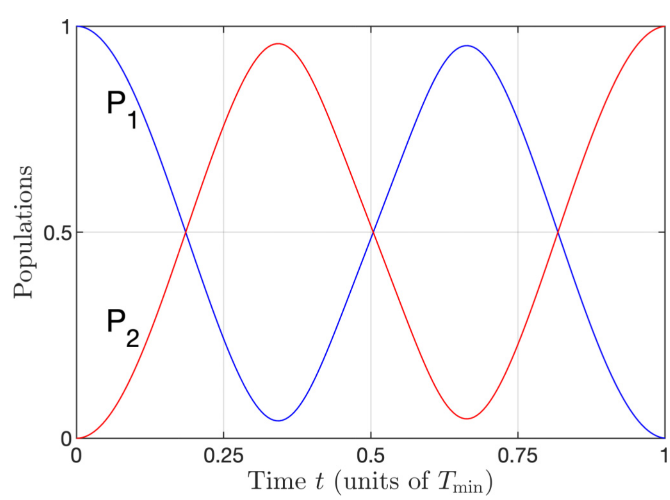

FIG. 3. Dynamics of the populations $P_j = |\langle j|\phi_\lambda(t_f)\rangle|^2$, $j = 1, 2$, corresponding to the time-optimal fifth-order robust complete population transfer (using the detuning shown in Fig. 2).

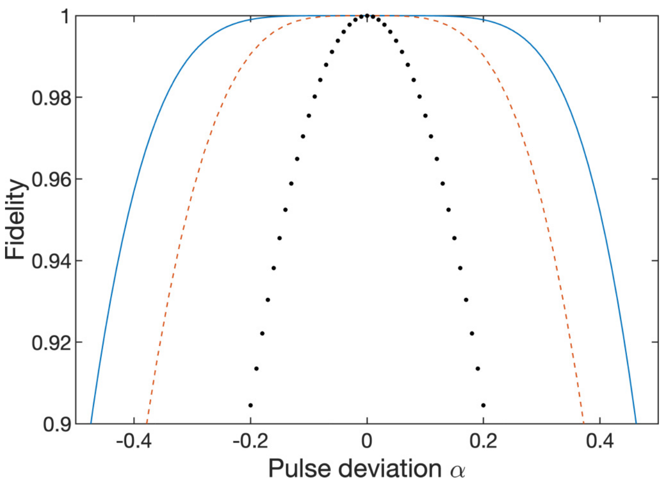

FIG. 4. Fidelity (transfer population P_2) of the optimal fifth-order (solid line) and third-order (dashed line) RIO complete population transfer compared to the Rabi profile (dotted line) as a function of the relative deviation of the pulse amplitude.

large-amplitude oscillations of the dynamics, reminiscent of the 3π-pulse Rabi oscillations. As expected, the fifth order features a significantly flatter profile than the third order (determined in [33]).

VI. ROBUST ARBITRARY GATE: NUMERICAL RESULTS

We consider the construction of the optimal fifth-order α-robust arbitrary SU(2) quantum gate as defined by (46) and parametrized by the (given) angle θ_0 and the two phases φ_0 and γ_0 and generated by the state (47) from the ground state.

A. Optimization with respect to energy or time

The boundaries read

$$\theta_i = 0, \quad \theta_f = \theta_0, \quad \gamma_i = \varphi_i = \pi/2, \quad \gamma_f = \gamma_0, \quad \varphi_f = \varphi_0 \tag{71}$$

and

$$|\dot{\theta}_i| = |\Omega_0|, \quad \dot{\gamma}_i = -\lambda_0/2 + \lambda_2/4. \tag{72}$$

We do not set $\gamma_0 = \gamma_f$ or $\varphi_0 = \varphi_f$; they result from the numerical calculation of the optimal solution giving γ_f and φ_f, respectively. We have determined systematically the six Lagrangian multipliers λ_0, λ_2, λ_3, λ_4, $\kappa_{x,i}$, and $\kappa_{y,i}$ and the minimum time for a given angle θ_0 in the range $[0.2, 1]\pi$, solving Eqs. (55) with the boundaries (71) and (72).

We started to determine the trajectory for the NOT-type gate $\theta_0 = \pi$,

$$U_{\mathrm{NOT};\kappa} = \begin{bmatrix} 0 & -e^{i\xi} \\ e^{-i\xi} & 0 \end{bmatrix}, \tag{73}$$

with $\xi \equiv (\varphi_0 + \gamma_0)/2$. We obtained two possible symmetric NOT trajectories with $\lambda_3 = \kappa_{y,i} = 0$, referred to as type 1 ($\lambda_0 \approx 3.250\Omega_0$, $\lambda_2 \approx 0.8988\Omega_0$, $\lambda_4 \approx 1.944\Omega_0$, and $\kappa_{x,i} \approx -3.510\Omega_0$) and type 2 ($\lambda_0 \approx 0.590\Omega_0$, $\lambda_2 \approx 0.8815\Omega_0$, $\lambda_4 \approx -1.974\Omega_0$, and $\kappa_{x,i} \approx -1.549\Omega_0$), respectively, of the same pulse area $\mathcal{A} \approx 4.20\pi$ and $\gamma_0 = \varphi_0 = \pi/2$, i.e., $\xi = \pi/2$. They are shown in Figs. 5 and 6, respectively.

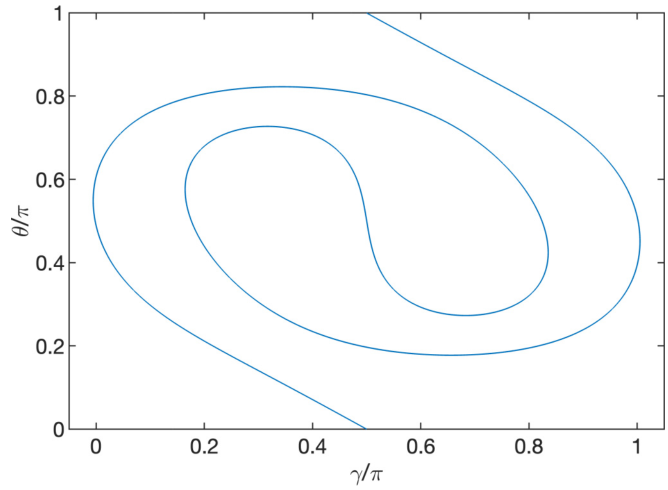

FIG. 5. Geodesic $\tilde{\theta}(\gamma)$ of type 1 corresponding to the optimal fifth-order α-robust NOT gate (see the text for details).

By continuity of the Lagrangian parameters, one can determine the trajectories for other values of θ_0, decreasing its value step by step from π. In practice, the search is much simpler when one alternatively decreases the final time $T_{\min}$, with which a given θ_0 is associated. For any given $\theta_0 < \pi$, we obtain that the trajectory continuously connected to the NOT trajectory of type 1 leads to a smaller final time $T_{\min}$. This set of trajectories is simply referred to as type-1 trajectories. For instance, for the Hadamard gate $\theta_0 = \pi/2$, one obtains $T_{\min} \approx 3.2/\Omega_0$ and $T_{\min} \approx 3.42/\Omega_0$ for types 1 and 2, respectively. The corresponding detunings are shown in Figs. 7 and 8, respectively. We thus retain the type-1 trajectories. The obtained Lagrangian multipliers, phases (which are numerically determined to be identical $\gamma_0 = \varphi_0$), and minimum times $T_{\min}$ for the type-1 trajectories are shown in Fig. 9. One can notice that the minimum time $T_{\min}$ increases linearly with respect to θ_0 as for the Rabi solution.

The resulting values of the phases $\gamma_0 = \varphi_0$ are given in Table II for some target SU(2) quantum gates parametrized by the angles θ_0. The pulse area decreases as a function of θ_0.

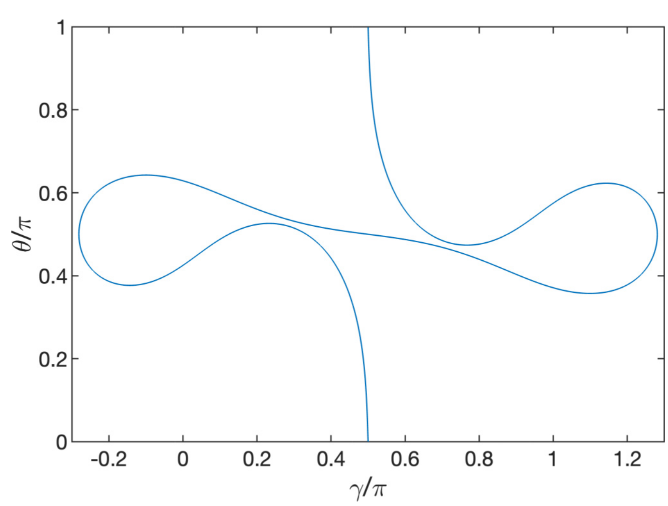

FIG. 6. Same as 5 but for the geodesic $\tilde{\theta}(\gamma)$ of type 2.

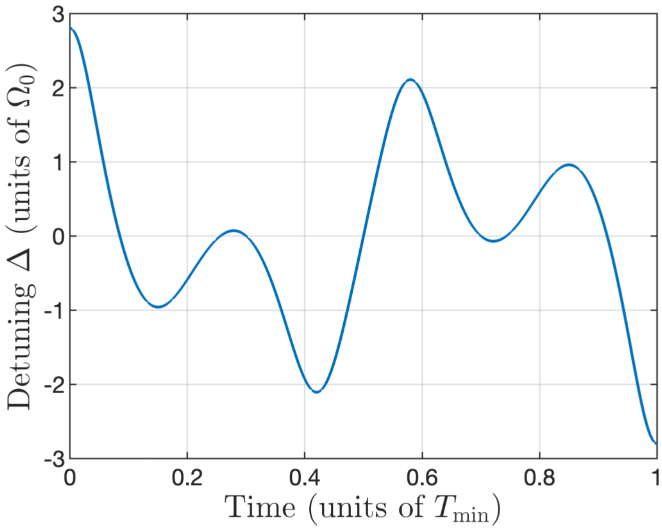

FIG. 7. Time-optimal detuning for the trajectory of Fig. 5.

As a particular example, the angle $\theta_0 = \pi/2$ corresponds to a Hadamard-type gate

$$U_{\mathrm{H};\varphi_0,\gamma_0} = \frac{1}{\sqrt{2}}\begin{bmatrix} e^{(i/2)(\varphi_0-\gamma_0)} & -e^{(i/2)(\varphi_0+\gamma_0)} \\ e^{-(i/2)(\varphi_0+\gamma_0)} & e^{-(i/2)(\varphi_0-\gamma_0)} \end{bmatrix}, \tag{74}$$

for which we obtain the off-diagonal phase $(\varphi_0 + \gamma_0)/2 \approx 1.065\pi$ and the diagonal phase $\varphi_0 - \gamma_0 = 0$ (from Table II). We determine numerically $\lambda_0 \approx 1.959$, $\lambda_2 \approx 1.746$, $\lambda_3 \approx -1.266$, $\lambda_4 \approx 3.305$, $\kappa_{x,i} \approx 5.473$, $\kappa_{y,i} \approx -7.157$, $\gamma_0 = \varphi_0 \approx 1.065\pi$, and the minimum time

$$T_{\min} \approx 3.20\pi/\Omega_0, \tag{75}$$

corresponding to a constant pulse of approximate total area of 3.20π. The resulting $\theta(t)$, $\gamma(t)$, detuning $\Delta(t)$, and dynamics are shown in Fig. 10. The resulting dynamics is shown in Fig. 10. One can notice the antisymmetric form of the detuning as for the third-order robust solution [33].

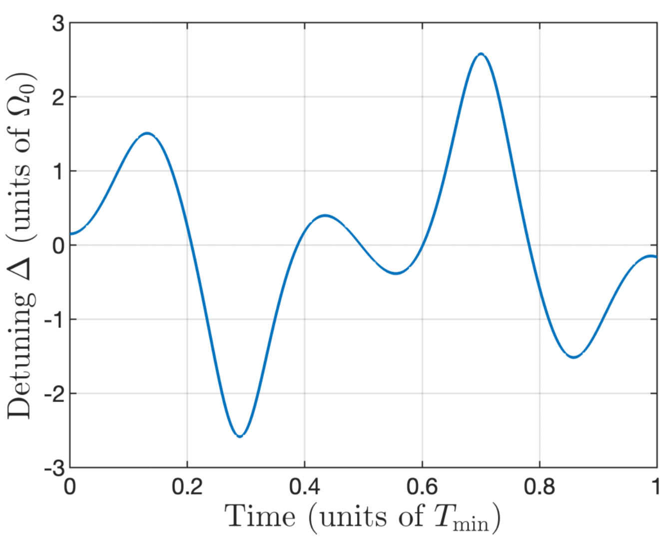

FIG. 8. Time-optimal detuning for the trajectory of Fig. 6.

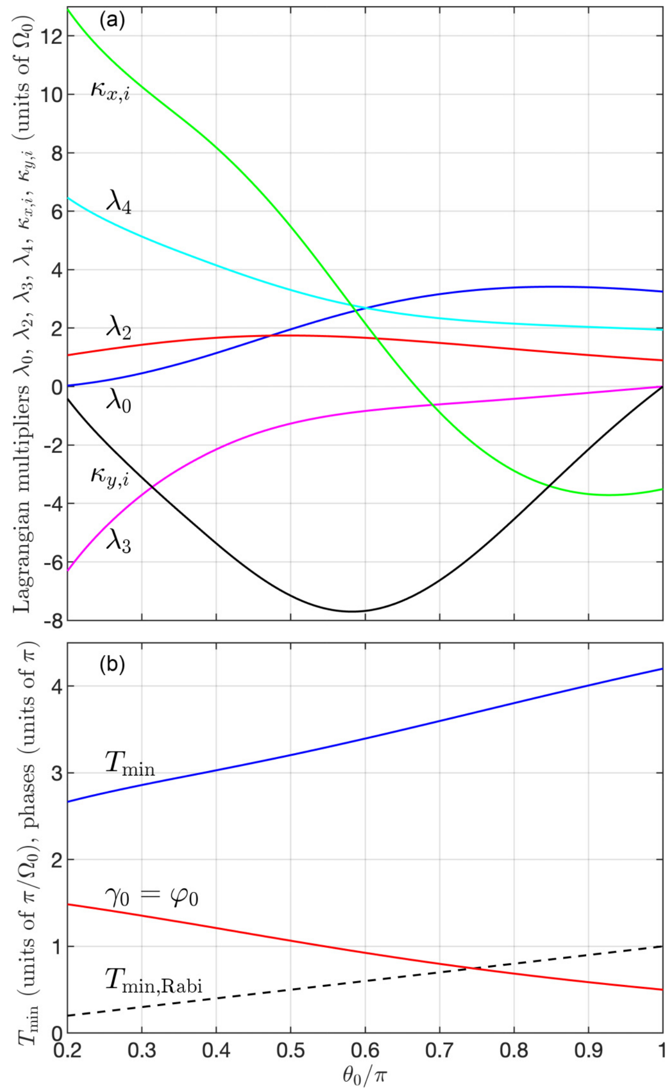

FIG. 9. (a) Lagrange multipliers and (b) corresponding optimal time and phases producing the fifth-order optimal robust gate as functions of θ_0 (type-1 trajectories; see Fig. 5 for the NOT gate). The curve of the (nonrobust) minimum time in the Rabi regime $T_{\min,\mathrm{Rabi}} = \theta_0/\Omega_0$ is shown as a dashed line for reference.

B. Comparison with the composite pulse technique

In this section the performance of the RIO approach is compared to the composite pulse (CP) technique. As

TABLE II. Approximate values of the phases $\gamma_0 = \varphi_0$ and pulse areas resulting from the optimization procedure for some fifth-order α-robust quantum gates parametrized by θ_0.

θ_0/π	$\gamma_0/\pi = \varphi_0/\pi$	Pulse area ($\times\pi$)
1/1000	1.50	1
1/10	1.53	2.37
1/4	1.42	2.77
1/2	1.065	3.20
3/4	0.740	3.70
1	1/2	4.20

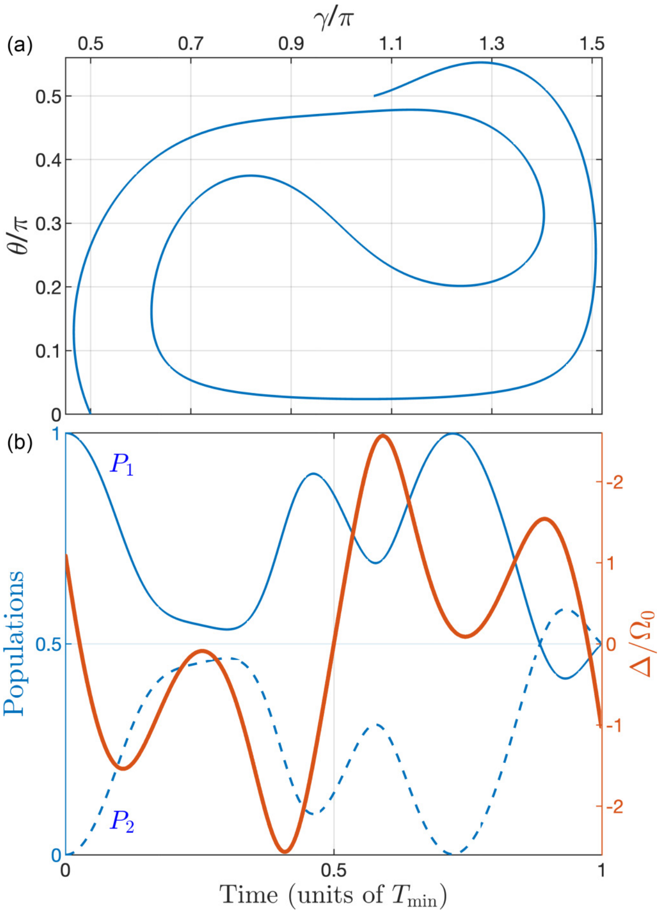

FIG. 10. (a) Optimal fifth-order α-robust geodesic $\tilde{\theta}(\gamma)$ for the Hadamard gate ($\theta_0 = \pi/2$) determined from numerical solution of (55). (b) Resulting detuning and dynamics of the populations P_j, $j = 1, 2$, realized from the ground state, for robust time-optimal control [obtained for a constant Rabi frequency Ω_0 according to (62)].

an illustrative example, we consider the fifth-order robust Hadamard gate (74) studied above, of pulse area $\Omega_0 T_{\min} \approx 3.20\pi$.

According to [14], the CP can be produced using a symmetric five-pulse sequence of respective areas (and phases as the index) $\omega_{\phi_1}\pi_{\phi_2}\pi_{\phi_3}\pi_{\phi_2}\omega_{\phi_1}$, with $\omega = 0.45\pi$, $\phi_1 = 1.9494\pi$, $\phi_2 = 0.5106\pi$, and $\phi_3 = 1.3179\pi$. This CP features the fastest total pulse area (3.9π) known so far in the literature for fifth-order α robustness. We conclude that RIO is considerably faster than the CP (18% faster). The robustness profile of RIO and of CP (both for fifth order) are shown in Fig. 11. We observe identical performances for ultrahigh fidelities (corresponding to an error below 10^{-4}). They are compared to third-order RIO and (first-order) Rabi techniques. The broadening of the curves for higher order is clearly demonstrated.

Concerning the NOT gate, the pulse area of the RIO method ($\mathcal{A} \approx 4.20\pi$) is 16% smaller than the best CP ($\mathcal{A} = 5\pi$) [14]. For gates with smaller targeted angles θ_0, the comparative performance of RIO increases since the total area of CP does not change much. For instance, RIO is 40% faster than CP for $\theta_0 = \pi/10$.

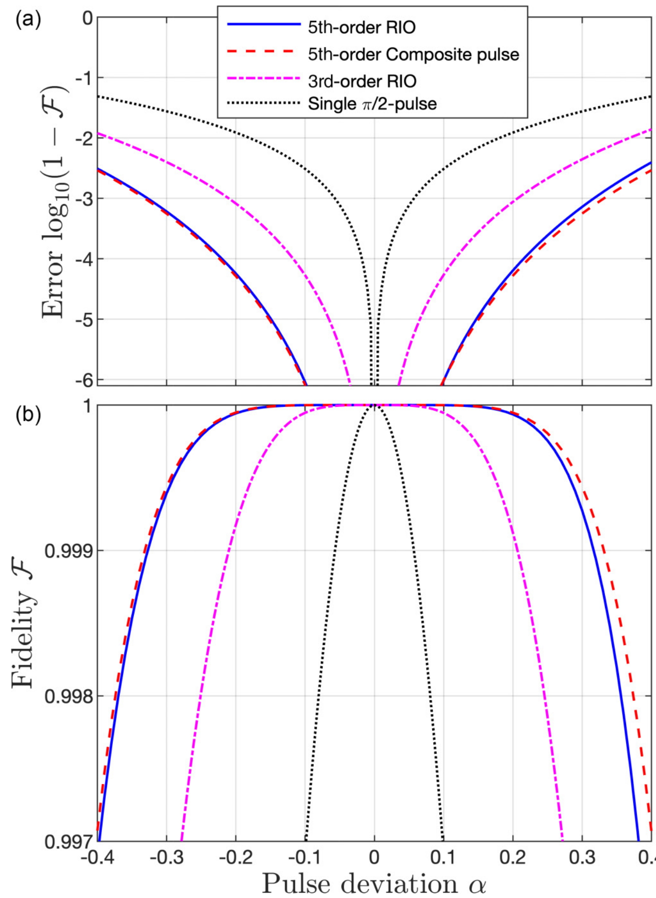

FIG. 11. (a) Fidelity and (b) infidelity in logarithmic scale of the Hadamard gate as a function of the pulse deviation α for RIO, CP, and Rabi techniques.

VII. OPTIMAL δ-ROBUST POPULATION TRANSFER

In this section we show that the problem of δ-robust optimal control (i.e., robust against inhomogeneous broadening of the frequencies or a slow stochastic noise in the energy level of the qubit) can be treated similarly. We consider the problem of complete population transfer and derive the corresponding differential equations by Euler-Lagrange optimization that optimally satisfy the cancellation of the integrals of the first element of Table I (at third order).

Nullification up to third order leads to

$$\int_{t_i}^{t_f} dt \sin\theta \cos\gamma = \int_{t_i}^{t_f} dt \sin\theta \sin\gamma = 0, \tag{76}$$

which corresponds to the two constraints rewritten as

$$\psi_1(\gamma,\theta) = \int_{t_i}^{t_f} dt \sin\theta \cos\gamma \equiv \int_{t_i}^{t_f} dt\, \varphi_1(\gamma,\theta) = 0, \tag{77a}$$

$$\psi_2(\gamma,\theta) = \int_{t_i}^{t_f} dt \sin\theta \sin\gamma \equiv \int_{t_i}^{t_f} dt\, \varphi_2(\gamma,\theta) = 0. \tag{77b}$$

Since the final phase is irrelevant for the population transfer problem, the final global phase γ_f is not considered.

For such a problem with uncertainty in the detuning, one cannot optimize with respect to pulse area, because this problem depends on the time parametrization (contrary to the α-robustness problem). We thus consider below the optimization with respect to a time-dependent cost, namely, the pulse energy or the time of the process itself.

A. Energy optimization

The problem can be formulated as an optimization problem: finding the trajectory $(\gamma(t), \theta(t))$ that minimizes the pulse energy

$$\mathcal{E}(\gamma,\theta) = \int_{t_i}^{t_f} dt(\dot{\theta}^2 + \dot{\gamma}^2 \sin^2\theta) \equiv \int_{t_i}^{t_f} dt\, \mathcal{L}_0(\dot{\gamma},\theta,\dot{\theta}) \tag{78}$$

under the two constraints (77).

1. General formulation

The problem can be solved by the Lagrange multiplier method: The trajectory $(\gamma(t), \theta(t))$ is the solution of

$$\mathrm{grad}\mathcal{E}(\gamma,\theta) + \lambda_1 \mathrm{grad}\psi_1(\gamma,\theta) + \lambda_2 \mathrm{grad}\psi_2(\gamma,\theta) = 0, \tag{79}$$

with λ_j, $j = 1, 2$, the Lagrangian multipliers associated with the constraints, where the gradient is defined as

$$\mathrm{grad}\mathcal{E}(\gamma,\theta) = \begin{bmatrix} \frac{\partial\mathcal{L}_0}{\partial\gamma} - \frac{d}{dt}\left(\frac{\partial\mathcal{L}_0}{\partial\dot{\gamma}}\right) \\ \frac{\partial\mathcal{L}_0}{\partial\theta} - \frac{d}{dt}\left(\frac{\partial\mathcal{L}_0}{\partial\dot{\theta}}\right) \end{bmatrix}, \tag{80a}$$

$$\mathrm{grad}\psi_j(\gamma,\theta) = \begin{bmatrix} \frac{\partial\varphi_j}{\partial\gamma} - \frac{d}{dt}\left(\frac{\partial\varphi_j}{\partial\dot{\gamma}}\right) \\ \frac{\partial\varphi_j}{\partial\theta} - \frac{d}{dt}\left(\frac{\partial\varphi_j}{\partial\dot{\theta}}\right) \end{bmatrix}. \tag{80b}$$

Equation (79) gives

$$-\frac{d}{dt}\left(\frac{\partial\mathcal{L}_0}{\partial\dot{\gamma}}\right) + \lambda_1\frac{\partial\varphi_1}{\partial\gamma} + \lambda_2\frac{\partial\varphi_2}{\partial\gamma} = 0, \tag{81a}$$

$$\frac{\partial\mathcal{L}_0}{\partial\theta} - \frac{d}{dt}\left(\frac{\partial\mathcal{L}_0}{\partial\dot{\theta}}\right) + \lambda_1\frac{\partial\varphi_1}{\partial\theta} + \lambda_2\frac{\partial\varphi_2}{\partial\theta} = 0, \tag{81b}$$

i.e.,

$$-2\frac{d}{dt}(\dot{\gamma}\sin^2\theta) + \sin\theta(\lambda_2\cos\gamma - \lambda_1\sin\gamma) = 0, \tag{82a}$$

$$2\dot{\gamma}^2\sin\theta\cos\theta - 2\frac{d}{dt}\dot{\theta} + \cos\theta(\lambda_1\cos\gamma + \lambda_2\sin\gamma) = 0, \tag{82b}$$

i.e.,

$$\ddot{\gamma}\sin\theta + 2\dot{\gamma}\dot{\theta}\cos\theta - \lambda_2\cos\gamma + \lambda_1\sin\gamma = 0, \tag{83a}$$

$$\dot{\gamma}^2\sin\theta\cos\theta - \ddot{\theta} + \cos\theta(\lambda_1\cos\gamma + \lambda_2\sin\gamma) = 0. \tag{83b}$$

We have divided in the equations above by a factor 2 and redefined the λ_j's accordingly. The problem can be solved numerically with the initial condition $\gamma(t_i) = \pi/2$, $\theta(t_i) = 0$, and $\dot{\gamma}(t_i)$ and $\dot{\theta}(t_i)$ both undefined at this stage.

2. Solution: Resonant pulse

The numerical solution of the system (83) gives $\lambda_1 = 0$, $\lambda_2 = 1$, and $\dot{\theta}_i \approx 1.142$ (in fact, since the problem appears to be singular when $\lambda_1 = 0$, we have to use numerically a small value for λ_1). Equation (83a) leads to

$$\ddot{\gamma}\sin\theta + 2\dot{\gamma}\dot{\theta}\cos\theta - \cos\gamma = 0, \tag{84}$$

of solution $\gamma = \pm\pi/2$, i.e., $\varphi = \pm\pi/2$ (independently of the sign of φ), $\dot{\theta} = \pm\Omega$ (where the $\pm$ sign is correlated with the sign of φ), and $\Delta = 0$ [28] (see Fig. 12). Equation (83b) gives then a differential equation similar to the pendulum equation of motion (if one shifts θ)

$$-\ddot{\theta} \pm \lambda\cos\theta = 0, \tag{85}$$

where the $\pm$ sign is correlated with the sign of $\sin\gamma$ and we have kept $\lambda \equiv \lambda_2$ for the normalization of the field (also associated with the value of $\dot{\theta}_i$). The constraint reduces to

$$\int_0^T dt\, \sin\theta(t)\sin\gamma(t) = 0, \tag{86}$$

where the final time is defined $t_f \equiv T$. We notice that $\sin\gamma$ has to change its sign at a time t_1 in order to satisfy the above constraint.

As shown in Appendix G, the angle $\theta(t)$ for time $t \in [0, t_1]$ is given by $\theta_+(t)$ of Eq. (G22), denoted by $\theta_0(t)$ and written in terms of the Jacobi amplitude function, the inverse of the incomplete elliptic integral

$$\theta_0(t) = 2\,\mathrm{am}(\omega t - F(\pi/4, m), m) + \frac{\pi}{2}, \tag{87}$$

with $\lambda = m\omega^2$ (G33), until $t = t_1$,

$$t_1 = \frac{2}{\omega}F(\pi/4, m), \tag{88}$$

for which $\theta(t_1) \equiv \theta_0(t_1) = \pi$. For time $t \in [t_1, t_2]$, we obtain [similar to (G39)]

$$\theta_1(t) = 2\,\mathrm{am}(-\omega t + F(\pi/4, m) + 2K(m), m) - \frac{\pi}{2}. \tag{89}$$

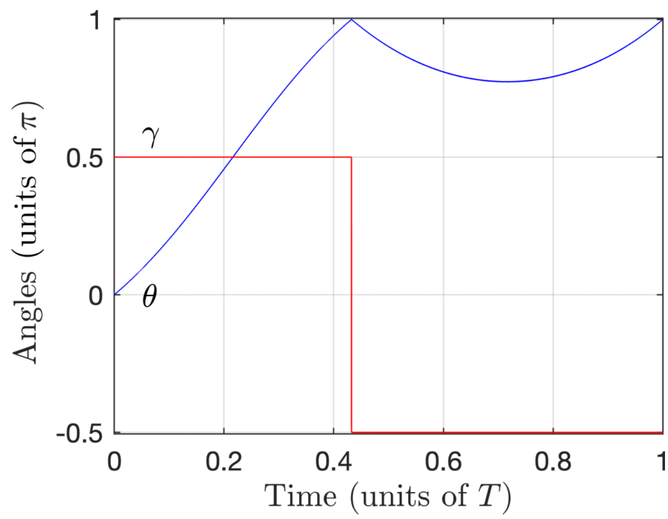

FIG. 12. Optimal robust geodesic $\theta(t)$ and $\gamma(t)$ for the complete population transfer robust with respect to the detuning with the final time $t_f = T \approx 4.219\,24/\omega$ (corresponding to $\lambda_2 = 1$ and $\lambda_1 = 0$). The time of the change of sign of $\sin\gamma$ is $t_1 \approx 0.4325T$. The time when $\dot{\theta} = 0$, corresponding to a zero field $\Omega = 0$, is $t_2 \approx 0.7162T$.

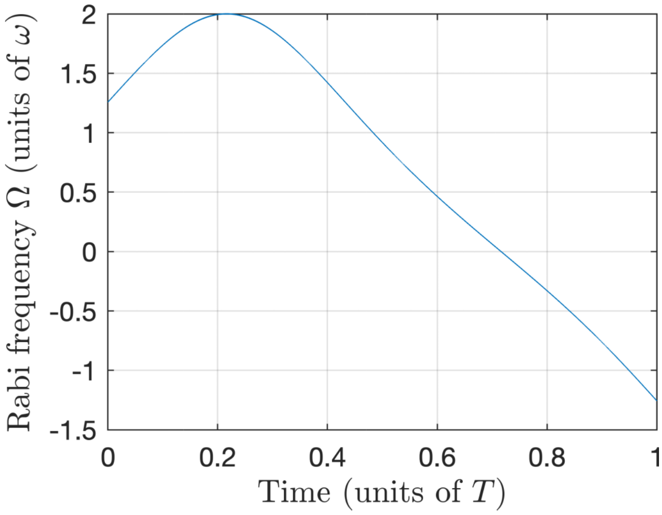

FIG. 13. Rabi frequency (94) corresponding to the angles of Fig. 12.

The subsequent negative part of the pulse for time $t \in [t_2, T]$ is given by $\theta_+(t)$ of Eq. (G30), denoted by $\theta_2(t)$ (G42),

$$\theta_2(t) = 2\,\mathrm{am}(\omega t + c_2'', m) - \frac{\pi}{2} \tag{90}$$

with

$$c_2'' = 2F(\arcsin(1/\sqrt{m}), m) - F(\pi/4, m) \tag{91}$$

until the final time

$$T = 2F(\arcsin(1/\sqrt{m}), m)/\omega. \tag{92}$$

The constraint that has to be satisfied reads

$$\int_0^{t_1} dt\,\sin\theta_0(t) - \int_{t_1}^{t_2} dt\,\sin\theta_1(t) - \int_{t_2}^{T} dt\,\sin\theta_2(t) = 0. \tag{93}$$

The pulse reads (G49)

$$\Omega(t) = 2\omega\,\mathrm{dn}(\omega t - F(\pi/4, m), m) \tag{94}$$

of peak $\Omega_0 = 2\omega$. We find numerically $m \approx 1.210\,485\,565\,4$, which satisfies (93). This gives the duration $T \approx 4.219\,24/\omega \approx 1.343\pi/\omega \approx 2.686\pi/\Omega_0$, the pulse energy $\mathcal{E} \approx 6.6623\omega \approx 3.331\,15\Omega_0$, and the pulse area (of the absolute value of Ω) $\mathcal{A} \approx 1.4523\pi$ (independent of ω). The corresponding angles, Rabi frequency, and dynamics of the populations are shown in Figs. 12–14, respectively. The transfer profile plotted in Fig. 15 shows the robustness of the process.

B. Time optimization

Minimization of the time corresponds to the Lagrangian

$$\int_{t_i}^{t_f} dt = T_{\min}, \quad \text{i.e., } \mathcal{L}_0 = 1. \tag{95}$$

In this case, we obtain

$$-\lambda_2\cos\gamma + \lambda_1\sin\gamma = 0, \tag{96a}$$

$$\cos\theta(\lambda_1\cos\gamma + \lambda_2\sin\gamma) = 0, \tag{96b}$$

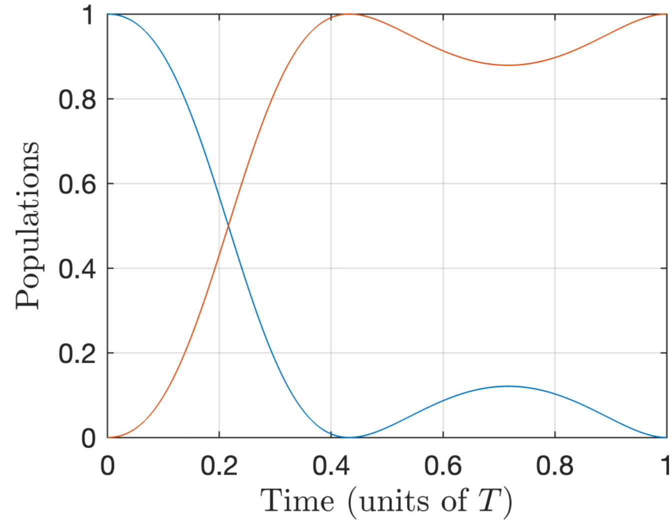

FIG. 14. Optimal robust population for the complete population transfer robust with respect to the detuning corresponding to the angles of Fig. 12.

which is satisfied for $\lambda_1 = \lambda_2 = 0$ since the determinant $\cos\theta(\sin^2\gamma + \cos^2\gamma) \neq 0$. We then take (as in the unconstraint case) a resonant pulse $\Delta = 0$, corresponding to $\varphi = \pm\pi/2$, $\gamma = \pi/2$, or $\gamma = 3\pi/2$, of constant amplitude of absolute value $\Omega_0 > 0$ [28]. This leads, at early times, for which we choose a positive field, to

$$\theta(t) = \theta_0(t) = \Omega_0 t, \tag{97}$$

with the constraint

$$\int_0^T dt\,\sin\theta(t)\sin\gamma(t) = 0. \tag{98}$$

We notice that $\sin\gamma$ has to change its sign at a time t_1 in order to satisfy the above constraint, i.e., as before, such that

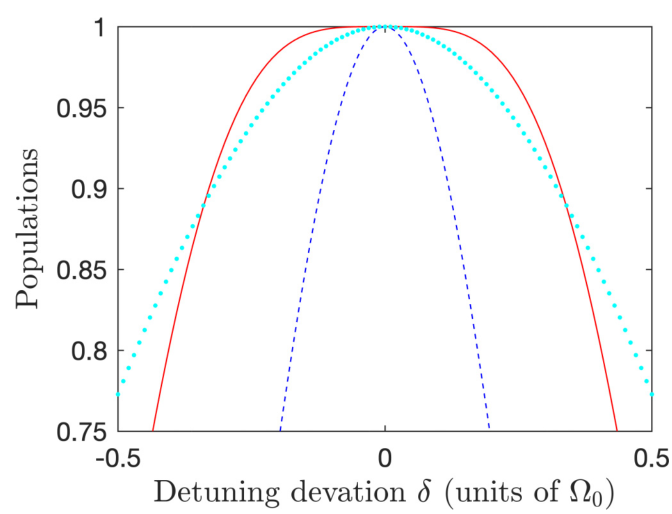

FIG. 15. Transfer profiles of the optimal complete population transfer robust with respect to the detuning from resonance (normalized with the peak Rabi frequency amplitude Ω_0) for energy (solid line) and time (dotted line) optimizations, respectively, compared to the Rabi π-pulse profile with a square pulse (dashed line).

$\Omega_0 t_1 = \pi$. At later times $t > t_1$, we have

$$\theta(t) = \theta_1(t) = 2\pi - \Omega_0 t, \tag{99}$$

satisfying the continuity $\theta_1(t_1) = \theta_0(t_1)$, until the pulse changes its sign at time t_2,

$$\theta(t) = \theta_2(t) = \Omega_0(t - 2t_2) + 2\pi \quad \text{for } t \in [t_2, T], \tag{100}$$

satisfying the continuity $\theta_2(t_2) = \theta_1(t_2)$ and finally $\theta_2(T) = \pi$, i.e., $T = 2t_2 - \pi/\Omega_0$. This leads to

$$\int_0^{t_2} dt \sin \Omega_0 t - \int_{t_2}^{T} dt \sin \Omega_0(t - 2t_2) = 0, \tag{101}$$

which gives

$$-\frac{1}{\Omega_0}[\cos \Omega_0 t]_0^{t_2} + \frac{1}{\Omega_0}[\cos \Omega_0(t - 2t_2)]_{t_2}^{T} = 0, \tag{102}$$

i.e.,

$$\cos \Omega_0 t_2 = 0. \tag{103}$$

The solution $\Omega_0 t_2 = 3\pi/2$ gives the final minimum time (in units of $1/\Omega_0$ that can be chosen at will)

$$T = 2\pi/\Omega_0 \tag{104}$$

and the bang pulse

$$\begin{aligned} \Omega(t) &= \Omega_0 \quad \text{for } t \in [0, t_2], \\ \Omega(t) &= -\Omega_0 \quad \text{for } t \in [t_2, T] \end{aligned} \tag{105}$$

of area $\mathcal{A} = 2\pi$ and energy $\mathcal{E} = 2\pi\Omega_0$. We notice that, for the same peak amplitudes, while the time of operation is 25% smaller than the one that minimizes the energy, the pulse area is 38% larger.

The transfer profiles comparing the efficiency of RIO for the energy and time optimization with the Rabi π-pulse transfer are shown in Fig. 15. The energy optimization appears more robust than the time optimization at the same order and with a lower pulse area.

VIII. CONCLUSION

In summary, we have formulated the RIO method in a systematic way in order to produce a robust control at any desired high order with respect to pulse inhomogeneities. Our analysis shows that the construction of a robust process up to an odd order $2n + 1$ (for a given integer n) only requires canceling the first n terms of the perturbative expansion (18) (for the population transfer) or (27) for the quantum gates (using the trace fidelity). We have applied the RIO method to generate optimal and ultrarobust arbitrary SU(2) quantum gates with respect to energy or time. Time α-robust optimization shows a constant Rabi coupling and a shaped detuning for any target.

The performance of RIO was compared to the composite technique. We then observed that RIO is considerably faster than CP, while having a similar performance. The detuning features a relatively simple shape with a dual-frequency oscillation (see Fig. 10). By comparison, the third order has a single-frequency (elliptic-cosine) form (see [33]).

Practical application in quantum computing requires an ultrahigh fidelity with a gate error typically not larger than 10^{-4}. The trace fidelity of the Hadamard shows then an admissible error in the pulse area of 10% at third order and of 20% at fifth order (see Fig. 11). For the more demanding Frobenius fidelity, the latter corresponds to an admissible error of 5% at second order. The pulse shaping of Fig. 8 is then recommended in practice to preserve ultrahigh fidelity despite such errors in the (global) pulse amplitude or duration.

An important question that can be treated by RIO concerns the additional constraint leading to a free single field parameter. We have seen that the α robustness for time minimization shows natural solutions with a constant coupling Ω (that can be chosen at will) and a variable detuning, while the lowest order of δ robustness shows a constant zero detuning (resonance) and a variable coupling. The constraint to a single parameter (due, e.g., to the experimental implementation) can be treated within RIO in general by adding a new integral characterizing this constraint in the angle coordinates. If one considers, for instance, the α robustness with a given pulse shape $\Omega(t)$, the angle $\gamma(t)$ is more specifically related to it via [30,35]

$$\int_{t_i}^{t} \Omega(s) ds = \int_{\gamma_i}^{\gamma(t)} d\gamma \sqrt{(\dot{\tilde{\theta}})^2 + \sin^2 \tilde{\theta}} \tag{106}$$

and the optimal detuning results from the optimal trajectory $\tilde{\theta}(\gamma)$. Another constraint consists in considering a constant detuning $\Delta = \Delta_0$ and a variable coupling $\Omega(t)$. This can be addressed via the rescaling of the coupling (for an arbitrary Ω_0)

$$s(t) = \frac{1}{\Omega_0} \int_0^t \Omega(s) ds, \quad \dot{s} = \Omega(t)/\Omega_0, \tag{107}$$

leading to the reduced problem

$$i \frac{\partial}{\partial s} |\tilde{\phi}(s)\rangle = \frac{1}{2} \begin{bmatrix} -\tilde{\Delta}(s) & \Omega_0 \\ \Omega_0 & \tilde{\Delta}(s) \end{bmatrix} |\tilde{\phi}(s)\rangle, \tag{108}$$

with

$$|\tilde{\phi}(s)\rangle = |\phi(t)\rangle, \quad \tilde{\Delta}(s) = \Delta_0/\Omega(t). \tag{109}$$

This leads to the optimization problem with an effective variable detuning and a constant coupling Ω_0, which has been treated in this paper. For α robustness, we have obtained a detuning necessarily passing by zero, which corresponds to an infinite coupling in the original problem. We conclude that a constant detuning and a variable coupling amplitude cannot achieve optimal α robustness.

The applicability of the RIO method requires (i) generating the dynamical invariants [36] associated with the symmetry of the problem, from which one can implement the inverse engineering technique [37,38], and (ii) finding the underlying Lagrangian multipliers (LMs). The dynamical invariants have been derived for SU(4) symmetry with interactions of the form $\sigma_i \otimes \sigma_i$, $\mathbb{1} \otimes \sigma_i$, and $\sigma_i \otimes \mathbb{1}$, $i = x, y, z$ [39], which covers most of the practical applications of quantum computation involving two-qubit operation. We notice that this does not limit the applicability to two-, three-, or four-level systems; higher dimensions with specific symmetries can be considered [40]. For instance, one can compensate for the error in the phase of a two-qubit controlled- PHASE gate using SU(2)-symmetry interactions $T_1 \equiv \frac{1}{2}\sigma_x \otimes \sigma_x$, $T_2 \equiv \frac{1}{2}\sigma_x \otimes \sigma_y$, and $T_3 \equiv \frac{1}{2}\mathbb{1} \otimes \sigma_z$

[41]. Concerning the LMs, we should be able to systematically process up to one-tenth of the LMs. Robustness with respect to field inhomogeneities (amplitude, duration, or pulse area) or inhomogeneous broadening (detuning) requires (i) two LMs for complete (or partial) population transfer and three LMs for single-qubit gate (if we consider the trace fidelity) at third order and (ii) four LMs for complete (or partial) population transfer and six LMs for single-qubit gate (if we consider the trace fidelity) at fifth order. If one considers robustness against both field inhomogeneities and inhomogeneous broadening, the number of LMs has to be multiplied by 2.

The RIO method is flexible and can be applied for various problems. For instance, one can consider robust ultrasmall excitation of a quantum transition needed in some applications of quantum technologies (e.g., for single-photon generation in cold atomic ensembles or doped solids by the Duan-Lukin-Cirac-Zoller protocol [42,43]), as it was recently proposed in the context of composite pulses [44]. One can then extend the search shown in Fig. 9 for θ_0 below 0.2π. For instance, we obtain a robust quantum gate with $\theta_0 \approx \pi/1000$ for $\Omega_0 T_{\min} = \pi$, which corresponds to an ultrasmall population transfer probability of approximately 2.5×10^{-6}.

The method developed in this paper can also be directly applied to take into account imperfections due to slow stochastic noises. It has to be considered in a quasistatic representation [29] or with adiabatic arguments. The RIO method has been recently applied for more general noise models [45].

ACKNOWLEDGMENTS

We acknowledge support from the EUR-EIPHI Graduate School (Grant No. 17-EURE-0002) and from the European Union's Horizon 2020 research and innovation program under the Marie Skłodowska-Curie Grant Agreement No. 765075 (LIMQUET).

APPENDIX A: CALCULATION OF THE INTEGRALS OF ROBUSTNESS

We calculate the integrals of robustness Q_n and O_n from their definition (15) and from the matrix products, symbolically written as [where we define $e \equiv e(t)$, $e' \equiv e(t')$, $e'' \equiv e(t'')$, etc., and in units such that $\hbar = 1$]

$$V_I V_I' = \begin{bmatrix} e & f \\ \bar{f} & -e \end{bmatrix}\begin{bmatrix} e' & f' \\ \bar{f}' & -e' \end{bmatrix} = \begin{bmatrix} ee' + f\bar{f}' & ef' - fe' \\ \bar{f}e' - e\bar{f}' & \bar{f}f' + ee' \end{bmatrix} \tag{A1}$$

and

$$V_I V_I' V_I'' = \begin{bmatrix} ee' + f\bar{f}' & ef' - fe' \\ \bar{f}e' - e\bar{f}' & \bar{f}f' + ee' \end{bmatrix}\begin{bmatrix} e'' & f'' \\ \bar{f}'' & -e'' \end{bmatrix} \tag{A2}$$

$$= \begin{bmatrix} (ee' + f\bar{f}')e'' + (ef' - fe')\bar{f}'' & \cdots \\ (\bar{f}e' - e\bar{f}')e'' + (\bar{f}f' + ee')\bar{f}'' & \cdots \end{bmatrix}, \tag{A3}$$

for Sec. III B. For the Q_n we obtain

$$|Q_1| = \left|\int_{t_i}^{t_f} dt\, f(t)\right|, \tag{A4a}$$

$$|Q_2| = \left|\int_{t_i}^{t_f} dt \int_{t_i}^{t} dt'[e(t)f(t') - f(t)e(t')]\right|$$
$$= \left|2\int_{t_i}^{t_f} dt\, e(t)\int_{t_i}^{t} dt' f(t') - \int_{t_i}^{t_f} dt\, f(t)\int_{t_i}^{t_f} dt\, e(t)\right|$$
$$= 2\left|\int_{t_i}^{t_f} dt\, e(t)\int_{t_i}^{t} dt' f(t')\right| \quad \text{when } Q_1 = 0, \tag{A4b}$$

$$|Q_3| = \left|\int_{t_i}^{t_f} dt \int_{t_i}^{t} dt' \int_{t_i}^{t'} dt''[f(t)e(t')e(t'') - e(t)f(t')e(t'') + f(t)\bar{f}(t')f(t'') + e(t)e(t')f(t'')]\right|$$
$$= \left|\frac{3}{2}\int_{t_i}^{t_f} dt\, f(t)\left(\int_{t_i}^{t} dt' e(t')\right)^2 - \int_{t_i}^{t_f} dt\, e(t)\int_{t_i}^{t_f} dt\, f(t)\int_{t_i}^{t} dt' e(t') + \int_{t_i}^{t_f} dt\, f(t)\int_{t_i}^{t_f} dt\, \bar{f}(t)\int_{t_i}^{t} dt' f(t') - \int_{t_i}^{t_f} dt\, \bar{f}(t)\left(\int_{t_i}^{t} dt' f(t')\right)^2 + \int_{t_i}^{t_f} dt\, e(t)\int_{t_i}^{t_f} dt\, e(t)\int_{t_i}^{t} dt' f(t') - \int_{t_i}^{t_f} dt\, e(t)\int_{t_i}^{t} dt' e(t')\int_{t_i}^{t} dt' f(t')\right|$$
$$= \left|2\int_{t_i}^{t_f} dt\, f(t)\left(\int_{t_i}^{t} dt' e(t')\right)^2 - \int_{t_i}^{t_f} dt\, e(t)\int_{t_i}^{t_f} dt\, f(t)\int_{t_i}^{t} dt' e(t') + \int_{t_i}^{t_f} dt\, f(t)\int_{t_i}^{t_f} dt\, \bar{f}(t)\int_{t_i}^{t} dt' f(t') - \int_{t_i}^{t_f} dt\, \bar{f}(t)\left(\int_{t_i}^{t} dt' f(t')\right)^2 + \int_{t_i}^{t_f} dt\, e(t)\int_{t_i}^{t_f} dt\, e(t)\int_{t_i}^{t} dt' f(t') - \int_{t_i}^{t_f} dt\, e(t)\int_{t_i}^{t} dt' e(t')\int_{t_i}^{t_f} dt' f(t')\right|$$
$$= \left|\int_{t_i}^{t_f} dt\left[2f(t)\left(\int_{t_i}^{t} dt' e(t')\right)^2 - \bar{f}(t)\left(\int_{t_i}^{t} dt' f(t')\right)^2\right]\right| \quad \text{when } Q_{m\leqslant 2} = 0, \tag{A4c}$$

using

$$\int_{t_i}^{t_f} dt\, f(t)\int_{t_i}^{t} dt' e(t')\int_{t_i}^{t'} dt'' e(t'') = \frac{1}{2}\int_{t_i}^{t_f} dt\, f(t)\left(\int_{t_i}^{t} dt' e(t')\right)^2, \tag{A5a}$$

$$\int_{t_i}^{t_f} dt\, e(t) \int_{t_i}^{t} dt' f(t') = \int_{t_i}^{t_f} dt\, e(t) \int_{t_i}^{t_f} dt\, f(t) - \int_{t_i}^{t_f} dt\, f(t) \int_{t_i}^{t} dt' e(t'). \tag{A5b}$$

One can rewrite the term Q_3 by applying integration by parts with $u'(t) = \bar{f}(t)$ and $v(t) = [\int_{t_i}^{t} dt' f(t')]^2$:

$$Q_3 = 2\left| \int_{t_i}^{t_f} dt \left[f(t)\left(\int_{t_i}^{t} dt' e(t') \right)^2 + \bar{f}(t) \left| \int_{t_i}^{t} dt' f(t') \right|^2 \right] \right|. \tag{A6}$$

For the O_n we obtain

$$|O_1| = \left| \int_{t_i}^{t_f} dt\, e(t) \right|, \tag{A7a}$$

$$\begin{aligned} |O_2| &= \left| \int_{t_i}^{t_f} dt \int_{t_i}^{t} dt' [e(t)e(t') + f(t)\bar{f}(t')] \right| \\ &= \left| \frac{1}{2}\left(\int_{t_i}^{t_f} dt\, e(t) \right)^2 + \frac{1}{2} \left| \int_{t_i}^{t_f} dt\, f(t) \right|^2 + i\,\mathrm{Im}\left(\int_{t_i}^{t_f} dt\, f(t) \int_{t_i}^{t} dt' \bar{f}(t') \right) \right| \\ &= \left| \int_{t_i}^{t_f} dt\, f(t) \int_{t_i}^{t} dt' \bar{f}(t') \right| \quad \text{when } O_1 = 0, \end{aligned} \tag{A7b}$$

$$= \left| \mathrm{Im}\left(\int_{t_i}^{t_f} dt\, f(t) \int_{t_i}^{t} dt' \bar{f}(t') \right) \right| \quad \text{when } O_1 = Q_1 = 0, \tag{A7c}$$

$$\begin{aligned} |O_3| &= \left| \int_{t_i}^{t_f} dt \int_{t_i}^{t} dt' \int_{t_i}^{t'} dt'' [e(t)e(t')e(t'') + f(t)\bar{f}(t')e(t'') + e(t)f(t')\bar{f}(t'') - f(t)e(t')\bar{f}(t'')] \right| \\ &= \left| \frac{1}{6}\left(\int_{t_i}^{t_f} e(t)dt \right)^3 + 2\int_{t_i}^{t_f} dt\, e(t) \left| \int_{t_i}^{t} dt' f(t') \right|^2 - \int_{t_i}^{t_f} dt\, e(t) \int_{t_i}^{t_f} dt \bar{f}(t) \int_{t_i}^{t} dt' f(t') + \int_{t_i}^{t_f} dt f(t) \int_{t_i}^{t_f} dt\, \bar{f}(t) \int_{t_i}^{t} dt' e(t') - \int_{t_i}^{t_f} dt\, f(t) \int_{t_i}^{t_f} dt\, e(t) \int_{t_i}^{t} dt' \bar{f}(t') \right| \\ &= 2\left| \int_{t_i}^{t_f} dt\, e(t) \left| \int_{t_i}^{t} dt' f(t') \right|^2 \right| \quad \text{when } O_1 = Q_1 = 0. \end{aligned} \tag{A7d}$$

APPENDIX B: OPTIMAL QUANTUM GATE TRAJECTORY WITH RESPECT TO PULSE AREA AT FIFTH ORDER

Canceling the terms of the propagator expansion (12) at first order, i.e., $\int_{t_i}^{t_f} dt\, e(t) = 0$ and $\int_{t_i}^{t_f} dt\, f(t) = 0$, and at the full second order, via (44c) and (40), the constraints become [where we use (44b) to satisfy $\int_{t_i}^{t_f} dt\, f(t) = 0$]

$$\psi_0(\tilde{\theta}) = \int_{\gamma_i}^{\gamma_f} d\gamma \sin^2\tilde{\theta} \equiv \int_{\gamma_i}^{\gamma_f} d\gamma\, \varphi_0(\tilde{\theta}) = 0, \tag{B1a}$$

$$\begin{aligned} \psi_1(\gamma,\tilde{\theta},\tilde{x}_\alpha,\tilde{y}_\alpha) &= \int_{\gamma_i}^{\gamma_f} d\gamma \left[\frac{1}{2}\sin 2\tilde{\theta}(\tilde{x}_\alpha\cos\gamma + \tilde{y}_\alpha\sin\gamma)\dot{\tilde{\theta}}(\tilde{x}_\alpha\sin\gamma - \tilde{y}_\alpha\cos\gamma) \right] \\ &\equiv \int_{\gamma_i}^{\gamma_f} d\gamma\, \varphi_1(\gamma,\tilde{\theta},\dot{\tilde{\theta}},\tilde{x}_\alpha,\tilde{y}_\alpha) = 0, \end{aligned} \tag{B1b}$$

$$\begin{aligned} \psi_2(\gamma,\tilde{\theta},\tilde{x}_\alpha,\tilde{y}_\alpha) &= \int_{\gamma_i}^{\gamma_f} d\gamma \left[\frac{1}{2}\sin 2\theta(\tilde{y}_\alpha\cos\gamma - \tilde{x}_\alpha\sin\gamma) + \dot{\tilde{\theta}}(\tilde{x}_\alpha\cos\gamma + \tilde{y}_\alpha\sin\gamma) \right] \\ &\equiv \int_{\gamma_i}^{\gamma_f} d\gamma\, \varphi_2(\gamma,\tilde{\theta},\dot{\tilde{\theta}},\tilde{x}_\alpha,\tilde{y}_\alpha) = 0, \end{aligned} \tag{B1c}$$

$$\psi_3(\gamma,\tilde{\theta},\tilde{x}_\alpha) = \int_{\gamma_i}^{\gamma_f} d\gamma\, \tilde{x}_\alpha \sin^2\tilde{\theta} \equiv \int_{\gamma_i}^{\gamma_f} d\gamma\, \varphi_3(\tilde{\theta},\tilde{x}_\alpha) = 0, \tag{B1d}$$

$$\psi_4(\gamma,\tilde{\theta},\tilde{y}_\alpha) = \int_{\gamma_i}^{\gamma_f} d\gamma\, \tilde{y}_\alpha \sin^2\tilde{\theta} \equiv \int_{\gamma_i}^{\gamma_f} d\gamma\, \varphi_4(\tilde{\theta},\tilde{y}_\alpha) = 0. \tag{B1e}$$

The trajectories $\tilde{\theta}(\gamma)$, $\tilde{x}_\alpha(\gamma)$, and $\tilde{y}_\alpha(\gamma)$ are the solution of the Euler-Lagrange equations

$$\frac{\partial\mathcal{L}}{\partial\tilde{\theta}} - \frac{d}{d\gamma}\left(\frac{\partial\mathcal{L}}{\partial\dot{\tilde{\theta}}} \right) = 0, \tag{B2a}$$

$$\frac{\partial\mathcal{L}}{\partial\tilde{x}_\alpha} - \frac{d}{d\gamma}\left(\frac{\partial\mathcal{L}}{\partial\dot{\tilde{x}}_\alpha} \right) = 0, \tag{B2b}$$

$$\frac{\partial\mathcal{L}}{\partial\tilde{y}_\alpha} - \frac{d}{d\gamma}\left(\frac{\partial\mathcal{L}}{\partial\dot{\tilde{y}}_\alpha} \right) = 0, \tag{B2c}$$

with

$$\begin{aligned} \mathcal{L}(\gamma,\tilde{\theta},\dot{\tilde{\theta}},\tilde{x}_\alpha,\dot{\tilde{x}}_\alpha,\tilde{y}_\alpha,\dot{\tilde{y}}_\alpha) &= \mathcal{L}_0(\tilde{\theta},\dot{\tilde{\theta}}) + \tilde{\lambda}_0\varphi_0(\tilde{\theta}) + \sum_{j=1,4}\tilde{\lambda}_j\varphi_j(\gamma,\tilde{\theta},\dot{\tilde{\theta}},\tilde{x}_\alpha,\tilde{y}_\alpha) \\ &\quad + \tilde{\mu}_x(\gamma)[\dot{\tilde{x}}_\alpha - \tilde{u}(\gamma,\tilde{\theta},\dot{\tilde{\theta}})] + \tilde{\mu}_y(\gamma)[\dot{\tilde{y}}_\alpha - \tilde{v}(\gamma,\tilde{\theta},\dot{\tilde{\theta}})]. \end{aligned} \tag{B3}$$

This gives

$$\begin{aligned} &\frac{\partial\mathcal{L}_0}{\partial\tilde{\theta}} - \frac{d}{d\gamma}\left(\frac{\partial\mathcal{L}_0}{\partial\dot{\tilde{\theta}}} \right) + \tilde{\lambda}_0\frac{\partial\varphi_0}{\partial\tilde{\theta}} + \sum_{j=1,4}\left[\tilde{\lambda}_j\frac{\partial\varphi_j}{\partial\tilde{\theta}} - \tilde{\lambda}_j\frac{d}{d\gamma}\left(\frac{\partial\varphi_j}{\partial\dot{\tilde{\theta}}} \right) \right] \\ &- \tilde{\mu}_x\frac{\partial\tilde{u}}{\partial\theta} - \tilde{\mu}_y\frac{\partial\tilde{v}}{\partial\theta} + \frac{d}{d\gamma}\left(\tilde{\mu}_x\frac{\partial\tilde{u}}{\partial\dot{\tilde{\theta}}} + \tilde{\mu}_y\frac{\partial\tilde{v}}{\partial\dot{\tilde{\theta}}} \right) = 0, \end{aligned} \tag{B4a}$$

$$\sum_{j=1,4} \tilde{\lambda}_j \frac{\partial \varphi_j}{\partial \tilde{x}_\alpha} - \dot{\tilde{\mu}}_x = 0, \tag{B4b}$$

$$\sum_{j=1,4} \tilde{\lambda}_j \frac{\partial \varphi_j}{\partial \tilde{y}_\alpha} - \dot{\tilde{\mu}}_y = 0, \tag{B4c}$$

i.e.,

$$\begin{aligned}
&\frac{2(\dot{\tilde{\theta}})^2\cot\tilde{\theta} + \sin\tilde{\theta}\cos\tilde{\theta} - \ddot{\tilde{\theta}}}{[(\dot{\tilde{\theta}})^2 + \sin^2\tilde{\theta}]^{3/2}} \\
&\quad + (2\tilde{\lambda}_0 - \tilde{\lambda}_2)\cot\tilde{\theta} - 2\tilde{\lambda}_2(\tilde{y}_\alpha\cos\gamma - \tilde{x}_\alpha\sin\gamma) \\
&\quad + \tilde{\lambda}_3\left(2\tilde{x}_\alpha\cot\tilde{\theta} + \frac{1}{2}\sin\gamma\right) + \tilde{\lambda}_4\left(2\tilde{y}_\alpha\cot\tilde{\theta} - \frac{1}{2}\cos\gamma\right) \\
&\quad - 2\tilde{\lambda}_1(\tilde{x}_\alpha\cos\gamma + \tilde{y}_\alpha\sin\gamma) + \tilde{\mu}_x\cos\gamma + \tilde{\mu}_y\sin\gamma = 0,
\end{aligned} \tag{B5a}$$

$$\dot{\tilde{\mu}}_x - 2\tilde{\lambda}_1\dot{\tilde{x}}_\alpha + 2\tilde{\lambda}_2\dot{\tilde{y}}_\alpha = \tilde{\lambda}_3\sin^2\tilde{\theta}, \tag{B5b}$$

$$\dot{\tilde{\mu}}_y - 2\tilde{\lambda}_1\dot{\tilde{y}}_\alpha - 2\tilde{\lambda}_2\dot{\tilde{x}}_\alpha = \tilde{\lambda}_4\sin^2\tilde{\theta}. \tag{B5c}$$

One can remove the $\tilde{\lambda}_1$ and simplify the above equations by defining

$$\tilde{\kappa}_x = \tilde{\mu}_x - 2\tilde{\lambda}_1\tilde{x}_\alpha + 2\tilde{\lambda}_2\tilde{y}_\alpha - \tfrac{1}{2}\tilde{\lambda}_4, \tag{B6a}$$

$$\tilde{\kappa}_y = \tilde{\mu}_y - 2\tilde{\lambda}_1\tilde{y}_\alpha - 2\tilde{\lambda}_2\tilde{x}_\alpha + \tfrac{1}{2}\tilde{\lambda}_3, \tag{B6b}$$

giving the complete system

$$\begin{aligned}
&\frac{2(\dot{\tilde{\theta}})^2\cot\tilde{\theta} + \sin\tilde{\theta}\cos\tilde{\theta} - \ddot{\tilde{\theta}}}{[(\dot{\tilde{\theta}})^2 + \sin^2\tilde{\theta}]^{3/2}} \\
&\quad + (2\tilde{\lambda}_0 - \tilde{\lambda}_2)\cot\tilde{\theta} + 2\tilde{\lambda}_2(\tilde{x}_\alpha\sin\gamma - \tilde{y}_\alpha\cos\gamma) \\
&\quad + (\tilde{\lambda}_3\tilde{x}_\alpha + \tilde{\lambda}_4\tilde{y}_\alpha)\cot\tilde{\theta} + \tilde{\kappa}_x\cos\gamma + \tilde{\kappa}_y\sin\gamma = 0,
\end{aligned} \tag{B7a}$$

$$\dot{\tilde{\kappa}}_x = \tilde{\lambda}_3\sin^2\tilde{\theta}, \quad \dot{\tilde{\kappa}}_y = \tilde{\lambda}_4\sin^2\tilde{\theta}, \tag{B7b}$$

$$\dot{\tilde{x}}_\alpha = \sin\tilde{\theta}\cos\tilde{\theta}\cos\gamma + \dot{\tilde{\theta}}\sin\gamma, \tag{B7c}$$

$$\dot{\tilde{y}}_\alpha = \sin\tilde{\theta}\cos\tilde{\theta}\sin\gamma - \dot{\tilde{\theta}}\cos\gamma, \tag{B7d}$$

with $\tilde{\kappa}_x(\gamma_i) = \kappa_{x,i}$, $\tilde{\kappa}_y(\gamma_i) = \kappa_{y,i}$, $\tilde{x}_\alpha(\gamma_i) = x_\alpha(t_i) = 0$, $\tilde{y}_\alpha(\gamma_i) = y_\alpha(t_i) = 0$, $\dot{\tilde{x}}_\alpha(\gamma_i) = \dot{\tilde{\theta}}_i\sin\gamma_i$, and $\dot{\tilde{y}}_\alpha(\gamma_i) = -\dot{\tilde{\theta}}_i\cos\gamma_i$ (where we have redefined $\tilde{x}_\alpha \to \tilde{x}_\alpha/2$ and $\tilde{y}_\alpha \to \tilde{y}_\alpha/2$).

APPENDIX C: OPTIMAL QUANTUM GATE TRAJECTORY WITH RESPECT TO ENERGY OR TIME AT FIFTH ORDER

The trajectories $\gamma(t)$, $\theta(t)$, $x_\alpha(t)$, and $y_\alpha(t)$ are the solution of the Euler-Lagrange equations (53), which can be written as

$$\begin{aligned}
&\frac{\partial\mathcal{L}_0}{\partial\gamma} - \frac{d}{dt}\left(\frac{\partial\mathcal{L}_0}{\partial\dot{\gamma}}\right) + \lambda_0\frac{\partial\varphi_0}{\partial\gamma} - \lambda_0\frac{d}{dt}\left(\frac{\partial\varphi_0}{\partial\dot{\gamma}}\right) \\
&\quad + \sum_{j=1}^{4}\left[\lambda_j\frac{\partial\varphi_j}{\partial\gamma} - \lambda_j\frac{d}{dt}\left(\frac{\partial\varphi_j}{\partial\dot{\gamma}}\right)\right] \\
&\quad -\mu_x\frac{\partial u}{\partial\gamma} - \mu_y\frac{\partial v}{\partial\gamma} + \frac{d}{dt}\left(\mu_x\frac{\partial u}{\partial\dot{\gamma}} + \mu_y\frac{\partial v}{\partial\dot{\gamma}}\right) = 0,
\end{aligned} \tag{C1a}$$

$$\begin{aligned}
&\frac{\partial\mathcal{L}_0}{\partial\theta} - \frac{d}{dt}\left(\frac{\partial\mathcal{L}_0}{\partial\dot{\theta}}\right) + \lambda_0\frac{\partial\varphi_0}{\partial\theta} - \lambda_0\frac{d}{dt}\left(\frac{\partial\varphi_0}{\partial\dot{\theta}}\right) \\
&\quad + \sum_{j=1}^{4}\left[\lambda_j\frac{\partial\varphi_j}{\partial\theta} - \lambda_j\frac{d}{dt}\left(\frac{\partial\varphi_j}{\partial\dot{\theta}}\right)\right] \\
&\quad - \mu_x\frac{\partial u}{\partial\theta} - \mu_y\frac{\partial v}{\partial\theta} + \frac{d}{dt}\left(\mu_x\frac{\partial u}{\partial\dot{\theta}} + \mu_y\frac{\partial v}{\partial\dot{\theta}}\right) = 0,
\end{aligned} \tag{C1b}$$

$$\lambda_1\frac{\partial\varphi_1}{\partial x_\alpha} + \lambda_2\frac{\partial\varphi_2}{\partial x_\alpha} + \lambda_3\frac{\partial\varphi_3}{\partial x_\alpha} + \lambda_4\frac{\partial\varphi_4}{\partial x_\alpha} - \dot{\mu}_x = 0, \tag{C1c}$$

$$\lambda_1\frac{\partial\varphi_1}{\partial y_\alpha} + \lambda_2\frac{\partial\varphi_2}{\partial y_\alpha} + \lambda_3\frac{\partial\varphi_3}{\partial y_\alpha} + \lambda_4\frac{\partial\varphi_4}{\partial y_\alpha} - \dot{\mu}_y = 0, \tag{C1d}$$

with, for optimization with respect to the pulse energy [according to (78)],

$$\mathcal{L}_0(\dot{\gamma},\theta,\dot{\theta}) = \dot{\theta}^2 + \dot{\gamma}^2\sin^2\theta \tag{C2a}$$

and

$$\varphi_0(\dot{\gamma},\theta) = \dot{\gamma}\sin^2\theta, \tag{C2b}$$

$$\begin{aligned}\varphi_1 &= \frac{\dot{\gamma}}{2}\sin 2\theta(x_\alpha\cos\gamma + y_\alpha\sin\gamma) \\ &\quad + \dot{\theta}(x_\alpha\sin\gamma - y_\alpha\cos\gamma),\end{aligned} \tag{C2c}$$

$$\begin{aligned}\varphi_2 &= \frac{\dot{\gamma}}{2}\sin 2\theta(y_\alpha\cos\gamma - x_\alpha\sin\gamma) \\ &\quad + \dot{\theta}(x_\alpha\cos\gamma + y_\alpha\sin\gamma),\end{aligned} \tag{C2d}$$

$$\varphi_3 = \dot{\gamma}x_\alpha\sin^2\theta, \tag{C2e}$$

$$\varphi_4 = \dot{\gamma}y_\alpha\sin^2\theta, \tag{C2f}$$

$$\dot{x}_\alpha = \frac{1}{4}\dot{\gamma}\sin 2\theta\cos\gamma + \frac{1}{2}\dot{\theta}\sin\gamma = u, \tag{C2g}$$

$$\dot{y}_\alpha = \frac{1}{4}\dot{\gamma}\sin 2\theta\sin\gamma - \frac{1}{2}\dot{\theta}\cos\gamma = v, \tag{C2h}$$

i.e.,

$$\begin{aligned}
&-2\ddot{\gamma}\sin^2\theta - 4\dot{\gamma}\dot{\theta}\sin\theta\cos\theta - 2\lambda_0\dot{\theta}\sin\theta\cos\theta \\
&\quad + 2\dot{\theta}\sin^2\theta[\lambda_1(x_\alpha\cos\gamma + y_\alpha\sin\gamma) \\
&\quad - \lambda_2(x_\alpha\sin\gamma - y_\alpha\cos\gamma)] \\
&\quad - \tfrac{1}{2}\sin 2\theta[(\lambda_1\cos\gamma - \lambda_2\sin\gamma)\dot{x}_\alpha \\
&\quad + (\lambda_1\sin\gamma + \lambda_2\cos\gamma)\dot{y}_\alpha] \\
&\quad - \lambda_3\dot{x}_\alpha\sin^2\theta - 2\lambda_3 x_\alpha\dot{\theta}\sin\theta\cos\theta \\
&\quad - \lambda_4\dot{y}_\alpha\sin^2\theta - 2\lambda_4 y_\alpha\dot{\theta}\sin\theta\cos\theta \\
&\quad - \dot{\theta}\sin^2\theta(\mu_x\cos\gamma + \mu_y\sin\gamma) \\
&\quad + \tfrac{1}{4}\sin 2\theta(\dot{\mu}_x\cos\gamma + \dot{\mu}_y\sin\gamma) = 0,
\end{aligned} \tag{C3a}$$

$$\begin{aligned}
&\dot{\gamma}^2\sin\theta\cos\theta - \ddot{\theta} + (\lambda_0 - \lambda_2/2)\dot{\gamma}\sin\theta\cos\theta \\
&\quad - \dot{\gamma}\sin^2\theta[\lambda_1(x_\alpha\cos\gamma + y_\alpha\sin\gamma) \\
&\quad + \lambda_2(y_\alpha\cos\gamma - x_\alpha\sin\gamma)] \\
&\quad + \dot{\gamma}\sin\theta\cos\theta(x_\alpha\lambda_3 + y_\alpha\lambda_4) \\
&\quad + \tfrac{1}{4}\dot{\gamma}\sin^2\theta(\lambda_3\sin\gamma - \lambda_4\cos\gamma) \\
&\quad + \tfrac{1}{2}\dot{\gamma}\sin^2\theta(\mu_x\cos\gamma + \mu_y\sin\gamma) = 0,
\end{aligned} \tag{C3b}$$

$$\begin{aligned}\dot{\mu}_x &= \lambda_1(\dot{\gamma}\cos\theta\sin\theta\cos\gamma+\dot{\theta}\sin\gamma)\\&\quad-\lambda_2(\dot{\gamma}\cos\theta\sin\theta\sin\gamma-\dot{\theta}\cos\gamma)+\lambda_3\dot{\gamma}\sin^2\theta\\&= 2\lambda_1\dot{x}_\alpha-2\lambda_2\dot{y}_\alpha+\lambda_3\dot{\gamma}\sin^2\theta, \quad\text{(C3c)}\\ \dot{\mu}_y &= \lambda_1(\dot{\gamma}\cos\theta\sin\theta\sin\gamma-\dot{\theta}\cos\gamma)\\&\quad+\lambda_2(\dot{\gamma}\cos\theta\sin\theta\cos\gamma+\dot{\theta}\sin\gamma)+\lambda_4\dot{\gamma}\sin^2\theta\\&= 2\lambda_1\dot{y}_\alpha+2\lambda_2\dot{x}_\alpha+\lambda_4\dot{\gamma}\sin^2\theta. \quad\text{(C3d)}\end{aligned}$$

One can remove the λ_1 and simplify the above equations by defining

$$\kappa_x = \mu_x - 2\lambda_1 x_\alpha + 2\lambda_2 y_\alpha - \tfrac{1}{2}\lambda_4, \quad\text{(C4a)}$$

$$\kappa_y = \mu_y - 2\lambda_1 y_\alpha - 2\lambda_2 x_\alpha + \tfrac{1}{2}\lambda_3, \quad\text{(C4b)}$$

which forms a system of six differential equations

$$\begin{aligned}&\ddot{\gamma}+2\dot{\gamma}\dot{\theta}\cot\theta+(\lambda_0-\lambda_2/2)\dot{\theta}\cot\theta\\&\quad+\dot{\theta}(\kappa_x\cos\gamma+\kappa_y\sin\gamma)+\lambda_2\dot{\theta}(x_\alpha\sin\gamma-y_\alpha\cos\gamma)\\&\quad+(\lambda_3x_\alpha+\lambda_4y_\alpha)\dot{\theta}\cot\theta=0, \quad\text{(C5a)}\\&\dot{\gamma}^2\sin\theta\cos\theta-\ddot{\theta}+(\lambda_0-\lambda_2/2)\dot{\gamma}\sin\theta\cos\theta\\&\quad+[\lambda_2(x_\alpha\sin\gamma-y_\alpha\cos\gamma)+\kappa_x\cos\gamma+\kappa_y\sin\gamma]\dot{\gamma}\sin^2\theta\\&\quad+(\lambda_3x_\alpha+\lambda_4y_\alpha)\dot{\gamma}\sin\theta\cos\theta=0, \quad\text{(C5b)}\end{aligned}$$

$$\dot{\kappa}_x = \lambda_3\dot{\gamma}\sin^2\theta, \quad\text{(C5c)}$$

$$\dot{\kappa}_y = \lambda_4\dot{\gamma}\sin^2\theta, \quad\text{(C5d)}$$

$$\dot{x}_\alpha = \dot{\gamma}\sin\theta\cos\theta\cos\gamma+\dot{\theta}\sin\gamma, \quad\text{(C5e)}$$

$$\dot{y}_\alpha = \dot{\gamma}\sin\theta\cos\theta\sin\gamma-\dot{\theta}\cos\gamma, \quad\text{(C5f)}$$

with the six Lagrangian multipliers $\lambda_0, \lambda_2, \lambda_3, \lambda_4, \kappa_{x,i}\equiv\kappa_x(t_i)$, and $\kappa_{y,i}\equiv\kappa_y(t_i)$ (where we have redefined $\kappa_x\to 2\kappa_x$, $\kappa_y\to 2\kappa_y$, $\lambda_3\to 2\lambda_3$, $\lambda_4\to 2\lambda_4$, $x_\alpha\to x_\alpha/2$, and $y_\alpha\to y_\alpha/2$) that define the optimal robust trajectory.

APPENDIX D: RECOVERING OPTIMAL TRAJECTORY WITH RESPECT TO PULSE AREA FROM ENERGY OPTIMIZATION AT FIFTH ORDER

We show below that we recover the trajectory defined by the differential equations (B7) for the minimization of the pulse area from the optimal trajectory with respect to energy, defined by Eqs. (55): Using $\dot{x}_\alpha = \dot{\tilde{x}}_\alpha\dot{\gamma}$ and $\dot{y}_\alpha = \dot{\tilde{y}}_\alpha\dot{\gamma}$, Eqs. (55e) and (55f) give (B7c) and (B7d), respectively. Using $\ddot{\theta} = \dot{\gamma}^2\ddot{\tilde{\theta}}+\ddot{\gamma}\dot{\tilde{\theta}}$, Eq. (55b) reads

$$\begin{aligned}&\dot{\gamma}\sin\theta\cos\theta-\dot{\gamma}\ddot{\tilde{\theta}}-\ddot{\gamma}\dot{\tilde{\theta}}/\dot{\gamma}+(\lambda_0-\lambda_2/2)\sin\theta\cos\theta\\&\quad+\sin^2\theta[\lambda_2(x_\alpha\sin\gamma-y_\alpha\cos\gamma)+\kappa_x\cos\gamma+\kappa_y\sin\gamma]\\&\quad+\sin\theta\cos\theta(\lambda_3x_\alpha+\lambda_4y_\alpha)=0, \quad\text{(D1)}\end{aligned}$$

which gives, using (55a) and $\dot{\theta} = \dot{\gamma}\dot{\tilde{\theta}}$,

$$\begin{aligned}&2(\dot{\tilde{\theta}})^2\cot\theta+\sin\theta\cos\theta-\ddot{\tilde{\theta}}+[(\lambda_0-\lambda_2/2)\cot\theta\\&\quad+\kappa_x\cos\gamma+\kappa_y\sin\gamma+\lambda_2(x_\alpha\sin\gamma-y_\alpha\cos\gamma)\\&\quad+\cot\theta(\lambda_3x_\alpha+\lambda_4y_\alpha)][(\dot{\tilde{\theta}})^2+\sin^2\theta]/\dot{\gamma}=0. \quad\text{(D2)}\end{aligned}$$

Using the constant of motion $\Omega_0^2 = \dot{\theta}^2+\dot{\gamma}^2\sin^2\theta = \dot{\gamma}^2[\sin^2\theta+(\dot{\tilde{\theta}})^2]$, i.e.,

$$\dot{\gamma} = \frac{\Omega_0}{\sqrt{\sin^2\theta+(\dot{\tilde{\theta}})^2}}, \quad\text{(D3)}$$

we recover (B7a), where we have identified the Lagrange multipliers

$$\begin{aligned}&\tilde{\lambda}_0=\lambda_0/2\Omega_0,\quad \tilde{\lambda}_2=\lambda_2/2\Omega_0,\quad \tilde{\lambda}_j=\lambda_j/\Omega_0,\quad j=3,4,\\&\tilde{\kappa}_x=\kappa_x/\Omega_0,\quad \tilde{\kappa}_y=\kappa_y/\Omega_0. \quad\text{(D4)}\end{aligned}$$

APPENDIX E: SYMMETRY OF THE TRAJECTORIES

1. Complete population transfer

We first invert the derivatives in order to get trajectories as a function of θ, $\tilde{\gamma}(\theta)$,

$$\dot{\tilde{\theta}} = \frac{d\tilde{\theta}}{d\gamma} = 1\Big/\left(\frac{d\tilde{\gamma}}{d\theta}\right) = 1/\dot{\tilde{\gamma}}, \quad\text{(E1a)}$$

$$\frac{d}{d\gamma}(\dot{\tilde{\theta}}\dot{\tilde{\gamma}}) = 0 = \ddot{\tilde{\theta}}\dot{\tilde{\gamma}}+\dot{\tilde{\theta}}\frac{d}{d\theta}(\dot{\tilde{\gamma}})\frac{d\tilde{\theta}}{d\gamma} = \ddot{\tilde{\theta}}\dot{\tilde{\gamma}}+(\dot{\tilde{\theta}})^2\ddot{\tilde{\gamma}}, \quad\text{(E1b)}$$

i.e.,

$$\ddot{\tilde{\theta}} = -\ddot{\tilde{\gamma}}/(\dot{\tilde{\gamma}})^3. \quad\text{(E2)}$$

We obtain, from (B7),

$$\begin{aligned}&\frac{2\dot{\tilde{\gamma}}\cot\theta+(\dot{\tilde{\gamma}})^3\sin\theta\cos\theta+\ddot{\tilde{\gamma}}}{[1+(\dot{\tilde{\gamma}})^2\sin^2\theta]^{3/2}}+2\tilde{\lambda}_2(\tilde{x}_\alpha\sin\tilde{\gamma}-\tilde{y}_\alpha\cos\tilde{\gamma})\\&\quad+\tilde{z}_\alpha\cot\theta+\tilde{\kappa}_x\cos\tilde{\gamma}+\tilde{\kappa}_y\sin\tilde{\gamma}=0, \quad\text{(E3a)}\end{aligned}$$

$$\dot{\tilde{\kappa}}_x = \dot{\tilde{\gamma}}\tilde{\lambda}_3\sin^2\theta,\quad \dot{\tilde{\kappa}}_y = \dot{\tilde{\gamma}}\tilde{\lambda}_4\sin^2\theta, \quad\text{(E3b)}$$

$$\begin{aligned}\dot{\tilde{z}}_\alpha &= \dot{\tilde{\gamma}}\sin\theta\cos\theta(\tilde{\lambda}_3\cos\tilde{\gamma}+\tilde{\lambda}_4\sin\tilde{\gamma})\\&\quad+\tilde{\lambda}_3\sin\tilde{\gamma}-\tilde{\lambda}_4\cos\tilde{\gamma}, \quad\text{(E3c)}\end{aligned}$$

with

$$\tilde{z}_\alpha = 2\tilde{\lambda}_0-\tilde{\lambda}_2+\tilde{\lambda}_3\tilde{x}_\alpha+\tilde{\lambda}_4\tilde{y}_\alpha \quad\text{(E4)}$$

and all the variables considered as functions of θ: $\tilde{z}_\alpha\equiv\tilde{z}_\alpha(\theta)$, etc. We analyze the problem of complete population transfer: $\tilde{\lambda}_0=\tilde{\lambda}_2=0$ and $\theta_f=\pi$. We consider the backward equations $\hat{\gamma}(u)=\tilde{\gamma}(\theta)$, $\hat{z}_\alpha(u)=\tilde{z}_\alpha(\theta)$, and $\hat{\kappa}_j(u)=\tilde{\kappa}_j(\theta)$, $j=x,y$, with $u=\pi-\theta$. This gives $\dot{\hat{\gamma}}=-\dot{\tilde{\gamma}}$, $\ddot{\hat{\gamma}}=\ddot{\tilde{\gamma}}$, $\dot{\hat{z}}_\alpha=-\dot{\tilde{z}}_\alpha$, $\ddot{\hat{z}}_\alpha=\ddot{\tilde{z}}_\alpha$, $\dot{\hat{\kappa}}_j=-\dot{\tilde{\kappa}}_j$, and $\ddot{\hat{\kappa}}_j=\ddot{\tilde{\kappa}}_j$. The resulting differential equations are of the same form as the original ones (E3) but with a change of sign of the derivative of $\hat{z}_\alpha$. As a consequence, the trajectory $\tilde{\gamma}(\theta)$ can be antisymmetric around $\theta=\pi/2$, $\tilde{\gamma}(\pi/2)\equiv\gamma_0=(\gamma_f+\gamma_i)/2=\gamma_f/2+\pi/4$ $(j=x,y)$, with antisymmetric functions $\tilde{\kappa}_j(\theta)$ and a symmetric function $\tilde{z}_\alpha(\theta)$,

$$\tilde{\gamma}(\pi-\theta) = 2\gamma_0-\tilde{\gamma}(\theta), \quad\text{(E5a)}$$

$$\dot{\tilde{\gamma}}(\pi-\theta)=\dot{\tilde{\gamma}}(\theta),\quad \ddot{\tilde{\gamma}}(\pi-\theta)=-\ddot{\tilde{\gamma}}(\theta), \quad\text{(E5b)}$$

$$\tilde{\kappa}_j(\pi-\theta)=2\kappa_{j,0}-\tilde{\kappa}_j(\theta),\quad \dot{\tilde{\kappa}}_j(\pi-\theta)=\dot{\tilde{\kappa}}_j(\theta), \quad\text{(E5c)}$$

$$\tilde{z}(\pi-\theta)=\tilde{z}(\theta),\quad \dot{\tilde{z}}(\pi-\theta)=-\dot{\tilde{z}}(\theta), \quad\text{(E5d)}$$

under the conditions determined below.

Taking the differential equation (E3) at $\theta = \pi - \theta_0$ and using the above equalities and (E3) at θ_0 gives

$$\begin{aligned}
&\tilde{\kappa}_x(\theta_0)\cos\tilde{\gamma}(\theta_0) + \tilde{\kappa}_y(\theta_0)\sin\tilde{\gamma}(\theta_0)\\
&\quad + \tilde{\kappa}_x(\pi-\theta_0)\cos[2\gamma_0 - \tilde{\gamma}(\theta_0)]\\
&\quad + \tilde{\kappa}_y(\pi-\theta_0)\sin[2\gamma_0 - \tilde{\gamma}(\theta_0)] = 0, \qquad \text{(E6a)}\\
&\sin\theta\cos\theta_0[\tilde{\lambda}_3\cos\tilde{\gamma}(\theta_0) + \tilde{\lambda}_4\sin\tilde{\gamma}(\theta_0)]\\
&\quad + [\tilde{\lambda}_3\sin\tilde{\gamma}(\theta_0) - \tilde{\lambda}_4\cos\tilde{\gamma}(\theta_0)]/\tilde{\gamma}(\dot{\theta}_0)\\
&\ = \sin\theta_0\cos\theta_0\{\tilde{\lambda}_3\cos[2\gamma_0 - \tilde{\gamma}(\theta_0)]\\
&\quad + \tilde{\lambda}_4\sin[2\gamma_0 - \tilde{\gamma}(\theta_0)]\} - \{\tilde{\lambda}_3\sin[2\gamma_0 - \tilde{\gamma}(\theta_0)]\\
&\quad - \tilde{\lambda}_4\cos[2\gamma_0 - \tilde{\gamma}(\theta_0)]\}/\dot{\tilde{\gamma}}(\theta_0) \qquad \text{(E6b)}
\end{aligned}$$

and Eq. (E6b) leads to

$$\tilde{\lambda}_3 = \tilde{\lambda}_4\cos\gamma_f - \tilde{\lambda}_3\sin\gamma_f, \qquad \text{(E7a)}$$

$$\tilde{\lambda}_4 = \tilde{\lambda}_3\cos\gamma_f + \tilde{\lambda}_4\sin\gamma_f, \qquad \text{(E7b)}$$

i.e., to the conditions

$$\cos\gamma_f = \frac{2\tilde{\lambda}_3\tilde{\lambda}_4}{(\tilde{\lambda}_3)^2 + (\tilde{\lambda}_4)^2}, \quad \sin\gamma_f = \frac{(\tilde{\lambda}_4)^2 - (\tilde{\lambda}_3)^2}{(\tilde{\lambda}_3)^2 + (\tilde{\lambda}_4)^2}. \qquad \text{(E8)}$$

Using the integration of Eqs. (B7b), Eq. (E6a) gives

$$\begin{aligned}
0 &= (\kappa_{x,i} + \kappa_{x,i}\sin\gamma_f - \kappa_{y,i}\cos\gamma_f)\cos[\tilde{\gamma}(\theta_0)]\\
&\quad + (\kappa_{y,i} - \kappa_{x,i}\cos\gamma_f - \kappa_{y,i}\sin\gamma_f)\sin[\tilde{\gamma}(\theta_0)]\\
&\quad + \int_0^{\theta_0} d\theta\,\sin^2\theta(\tilde{\lambda}_3 + \tilde{\lambda}_3\sin\gamma_f - \tilde{\lambda}_4\cos\gamma_f)\cos[\tilde{\gamma}(\theta_0)]\\
&\quad + \int_0^{\theta_0} d\theta\,\sin^2\theta(\tilde{\lambda}_4 - \tilde{\lambda}_3\cos\gamma_f - \lambda_4\sin\gamma_f)\sin[\tilde{\gamma}(\theta_0)]\\
&\quad + 2(\kappa_{x,0}\cos\gamma_f + \kappa_{y,0}\sin\gamma_f)\sin[\tilde{\gamma}(\theta_0)]\\
&\quad + 2(\kappa_{y,0}\cos\gamma_f - \kappa_{x,0}\sin\gamma_f)\cos[\tilde{\gamma}(\theta_0)], \qquad \text{(E9)}
\end{aligned}$$

which using (E7) simplifies to

$$\kappa_{x,i} = (\kappa_{y,i} - 2\kappa_{y,0})\cos\gamma_f - (\kappa_{x,i} - 2\kappa_{x,0})\sin\gamma_f, \quad \text{(E10a)}$$

$$\kappa_{y,i} = (\kappa_{x,i} - 2\kappa_{x,0})\cos\gamma_f + (\kappa_{y,i} - 2\kappa_{y,0})\sin\gamma_f, \quad \text{(E10b)}$$

which complete the conditions (E8) for the antisymmetric trajectory (E5).

2. The NOT gate

We assume an antisymmetric $\theta(t)$ around $\theta(T/2) = \pi/2$ (defining $T = T_{\min}$),

$$\theta(T-t) = \pi - \theta(t), \qquad \text{(E11a)}$$

$$\dot{\theta}(T-t) = \dot{\theta}(t), \quad \ddot{\theta}(T-t) = -\ddot{\theta}(t). \qquad \text{(E11b)}$$

a. Antisymmetric $\gamma(t)$

We additionally assume an antisymmetric $\gamma(t)$ around $\gamma_0 \equiv \gamma(T/2) = (\gamma_f + \gamma_i)/2 = \gamma_f/2 + \pi/4$:

$$\gamma(T-t) = 2\gamma_0 - \gamma(t), \qquad \text{(E12a)}$$

$$\dot{\gamma}(T-t) = \dot{\gamma}(t), \quad \ddot{\gamma}(T-t) = -\ddot{\gamma}(t). \qquad \text{(E12b)}$$

We consider Eqs. (55) at time $T - t$. From (55e) and (55f) we have, when $\gamma_0 = \gamma_f = \pi/2$, $\dot{x}_\alpha$ symmetric $\dot{x}_\alpha(T-t) = \dot{x}_\alpha(t)$ and $\dot{y}_\alpha$ antisymmetric $\dot{y}_\alpha(T-t) = -\dot{y}_\alpha(t)$, i.e., x_α antisymmetric $x_\alpha(T-t) = -x_\alpha(t)$ and y_α symmetric $y_\alpha(T-t) = y_\alpha(t)$.

From (55c) and (55d) we have both $\dot{\kappa}_x$ and $\dot{\kappa}_y$ symmetric $\kappa_j(T-t) = 2\kappa_{j,0} - \kappa_j(t)$. From (55a) and (55b) at time $T - t$, we show that Eqs. (55a) and (55b) are recovered at time t if $\kappa_x = \text{const}$, i.e., $\lambda_3 = 0$, and $\kappa_{y,0} = 0$.

b. Symmetric $\gamma(t)$

Alternatively, we consider a symmetric $\gamma(t)$ around $\gamma(T/2)$:

$$\gamma(T-t) = \gamma(t), \qquad \text{(E13a)}$$

$$\dot{\gamma}(T-t) = -\dot{\gamma}(t), \quad \ddot{\gamma}(T-t) = \ddot{\gamma}(t). \qquad \text{(E13b)}$$

From (55e) and (55f) we have both $\dot{x}_\alpha$ and $\dot{y}_\alpha$ symmetric $x_\alpha(T-t) = -x_\alpha(t)$ and $y_\alpha(T-t) = -y_\alpha(t)$. From (55c) and (55d) we have both $\dot{\kappa}_x$ and $\dot{\kappa}_y$ antisymmetric $\kappa_j(T-t) = \kappa_j(t)$. From (55a) and (55b) at time $T-t$, we show that Eqs. (55a) and (55b) are recovered at time t if $\lambda_0 = \lambda_2 = 0$. We have not found any RIO solution for the NOT gate satisfying these conditions.

APPENDIX F: ALTERNATIVE FORMULATION OF OPTIMIZATION OF ROBUST POPULATION TRANSFER WITH RESPECT TO ENERGY AND TIME AT FIFTH ORDER

We consider the constraint $\int_{t_i}^{t_f} f(t)dt = 0$, rewritten after integration by parts

$$\int_{t_i}^{t_f} dt\,\dot{\gamma}(\sin 2\theta - 2\theta)e^{i\gamma} - 2i(\theta_f e^{i\gamma_f} - \theta_i e^{i\gamma_i}) = 0, \qquad \text{(F1)}$$

giving

$$\begin{aligned}
\psi_1(\gamma,\theta) &\equiv \int_{t_i}^{t_f} dt\,\dot{\gamma}\cos\gamma(\sin 2\theta - 2\theta)\\
&\equiv \int_{t_i}^{t_f} dt\,\varphi_1(\gamma,\dot{\gamma},\theta) = -2\theta_f\sin\gamma_f, \qquad \text{(F2a)}\\
\psi_2(\gamma,\theta) &\equiv \int_{t_i}^{t_f} dt\,\dot{\gamma}\sin\gamma(\sin 2\theta - 2\theta)\\
&\equiv \int_{t_i}^{t_f} dt\,\varphi_2(\gamma,\dot{\gamma},\theta) = 2\theta_f\cos\gamma_f, \qquad \text{(F2b)}
\end{aligned}$$

and the integrals (40), i.e., (50e) and (50f). The constraint $\int_{t_i}^{t_f} f(t)dt = 0$ also has to be applied to these variables:

$$x_\alpha(t_f) = 0, \quad y_\alpha(t_f) = 0. \qquad \text{(F3)}$$

The trajectories $\gamma(t)$, $\theta(t)$, $x_\alpha(t)$, and $y_\alpha(t)$ are the solution of the Euler-Lagrange equations with

$$\begin{aligned}
\mathcal{L} &= \mathcal{L}_0(\dot{\gamma},\theta,\dot{\theta}) + \sum_{j=1}^{2}\lambda_j\varphi_j(\gamma,\dot{\gamma},\theta) + \lambda_3\varphi_3(\dot{\gamma},\theta,x_\alpha)\\
&\quad + \lambda_4\varphi_4(\dot{\gamma},\theta,y_\alpha) + \mu_x(t)[\dot{x}_\alpha - u(\gamma,\dot{\gamma},\theta,\dot{\theta})]\\
&\quad + \mu_y(t)[\dot{y}_\alpha - v(\gamma,\dot{\gamma},\theta,\dot{\theta})]. \qquad \text{(F4)}
\end{aligned}$$

This gives

$$-\frac{d}{dt}\left(\frac{\partial\mathcal{L}_0}{\partial\dot\gamma}\right) + \sum_{j=1}^{2}\left[\lambda_j\frac{\partial\varphi_j}{\partial\gamma}-\lambda_j\frac{d}{dt}\left(\frac{\partial\varphi_j}{\partial\dot\gamma}\right)\right]-\sum_{j=3}^{4}\lambda_j\frac{d}{dt}\left(\frac{\partial\varphi_j}{\partial\dot\gamma}\right) - \mu_x\frac{\partial u}{\partial\gamma}-\mu_y\frac{\partial v}{\partial\gamma}+\frac{d}{dt}\left(\mu_x\frac{\partial u}{\partial\dot\gamma}+\mu_y\frac{\partial v}{\partial\dot\gamma}\right)=0, \quad \text{(F5a)}$$

$$\frac{\partial\mathcal{L}_0}{\partial\theta}-\frac{d}{dt}\left(\frac{\partial\mathcal{L}_0}{\partial\dot\theta}\right)+\sum_{j=1}^{4}\lambda_j\frac{\partial\varphi_j}{\partial\theta} - \mu_x\frac{\partial u}{\partial\theta}-\mu_y\frac{\partial v}{\partial\theta}+\frac{d}{dt}\left(\mu_x\frac{\partial u}{\partial\dot\theta}+\mu_y\frac{\partial v}{\partial\dot\theta}\right)=0, \quad \text{(F5b)}$$

$$\lambda_3\frac{\partial\varphi_3}{\partial x_\alpha}-\dot\mu_x=0,\quad \lambda_4\frac{\partial\varphi_4}{\partial y_\alpha}-\dot\mu_y=0, \quad \text{(F5c)}$$

with

$$\mathcal{L}_0(\dot\gamma,\theta,\dot\theta)=\dot\theta^2+\dot\gamma^2\sin^2\theta, \quad \text{(F6a)}$$

$$\varphi_1(\gamma,\dot\gamma,\theta)=\dot\gamma\cos\gamma(\sin 2\theta-2\theta), \quad \text{(F6b)}$$

$$\varphi_2(\gamma,\dot\gamma,\theta)=\dot\gamma\sin\gamma(\sin 2\theta-2\theta), \quad \text{(F6c)}$$

$$\varphi_3(\dot\gamma,\theta,x_\alpha)=\dot\gamma x_\alpha\sin^2\theta, \quad \text{(F6d)}$$

$$\varphi_4(\dot\gamma,\theta,y_\alpha)=\dot\gamma y_\alpha\sin^2\theta, \quad \text{(F6e)}$$

$$\dot x_\alpha=\tfrac14\dot\gamma\sin 2\theta\cos\gamma+\tfrac12\dot\theta\sin\gamma=u, \quad \text{(F6f)}$$

$$\dot y_\alpha=\tfrac14\dot\gamma\sin 2\theta\sin\gamma-\tfrac12\dot\theta\cos\gamma=v, \quad \text{(F6g)}$$

i.e.,

$$\ddot\gamma\sin^2\theta+2\dot\gamma\dot\theta\sin\theta\cos\theta-2\dot\theta\sin^2\theta(\lambda_1\cos\gamma+\lambda_2\sin\gamma) +\tfrac12\sin^2\theta(\lambda_3\dot x_\alpha+\lambda_4\dot y_\alpha)+\dot\theta\sin\theta\cos\theta(\lambda_3x_\alpha+\lambda_4y_\alpha) +\tfrac12\dot\theta\sin^2\theta(\mu_x\cos\gamma+\mu_y\sin\gamma) -\tfrac14\sin\theta\cos\theta(\dot\mu_x\cos\gamma+\dot\mu_y\sin\gamma)=0, \quad \text{(F7a)}$$

$$\dot\gamma^2\sin\theta\cos\theta-\ddot\theta-2\dot\gamma\sin^2\theta(\lambda_1\cos\gamma+\lambda_2\sin\gamma) +\tfrac12\dot\gamma\sin 2\theta(\lambda_3x_\alpha+\lambda_4y_\alpha)+\tfrac14\dot\mu_x\sin\gamma-\tfrac14\dot\mu_y\cos\gamma +\tfrac12\dot\gamma\sin^2\theta(\mu_x\cos\gamma+\mu_y\sin\gamma)=0, \quad \text{(F7b)}$$

$$\dot\mu_x=\lambda_3\dot\gamma\sin^2\theta,\quad \dot\mu_y=\lambda_4\dot\gamma\sin^2\theta. \quad \text{(F7c)}$$

One can simplify by removing λ_1 and λ_2,

$$\ddot\gamma\sin\theta+2\dot\gamma\dot\theta\cos\theta +\tfrac12\dot\theta\sin\theta(\kappa_x\cos\gamma+\kappa_y\sin\gamma)+\dot\theta z_\alpha\cos\theta=0, \quad \text{(F8a)}$$

$$\dot\gamma^2\cos\theta-\ddot\theta/\sin\theta +\tfrac12\dot\gamma\sin\theta(\kappa_x\cos\gamma+\kappa_y\sin\gamma)+\dot\gamma z_\alpha\cos\theta=0, \quad \text{(F8b)}$$

with

$$\kappa_x=\mu_x-4\lambda_1-\tfrac12\lambda_4,\quad \kappa_y=\mu_y-4\lambda_2+\tfrac12\lambda_3, \quad \text{(F9a)}$$

$$z_\alpha=\lambda_3x_\alpha+\lambda_4y_\alpha,\quad z_\alpha(t_i)=z_\alpha(t_f)=0, \quad \text{(F9b)}$$

i.e.,

$$\dot\kappa_x=\dot\mu_x=\lambda_3\dot\gamma\sin^2\theta,\quad \dot\kappa_y=\dot\mu_y=\lambda_4\dot\gamma\sin^2\theta, \quad \text{(F10a)}$$

$$\dot z_\alpha=\tfrac12\dot\gamma\sin\theta\cos\theta(\lambda_3\cos\gamma+\lambda_4\sin\gamma) +\tfrac12\dot\theta(\lambda_3\sin\gamma-\lambda_4\cos\gamma). \quad \text{(F10b)}$$

Rewriting $\kappa_x\to2\kappa_x$, $\kappa_y\to2\kappa_y$, $\lambda_3\to2\lambda_3$, and $\lambda_4\to2\lambda_4$ in (F8) and (F10), we finally derive the system of five differential equations that define the optimal robust trajectory

$$\ddot\gamma\sin\theta+2\dot\gamma\dot\theta\cos\theta +\dot\theta(\kappa_x\cos\gamma+\kappa_y\sin\gamma)\sin\theta+\dot\theta z_\alpha\cos\theta=0, \quad \text{(F11a)}$$

$$-\ddot\theta/\sin\theta+\dot\gamma^2\cos\theta +\dot\gamma(\kappa_x\cos\gamma+\kappa_y\sin\gamma)\sin\theta+\dot\gamma z_\alpha\cos\theta=0, \quad \text{(F11b)}$$

$$\dot\kappa_x=\lambda_3\dot\gamma\sin^2\theta,\quad \dot\kappa_y=\lambda_4\dot\gamma\sin^2\theta, \quad \text{(F11c)}$$

$$\dot z_\alpha=(\lambda_3\cos\gamma+\lambda_4\sin\gamma)\dot\gamma\sin\theta\cos\theta +(\lambda_3\sin\gamma-\lambda_4\cos\gamma)\dot\theta, \quad \text{(F11d)}$$

with the four Lagrangian multipliers λ_3, λ_4, $\kappa_{0x}\equiv\kappa_x(t_i)$, and $\kappa_{0y}\equiv\kappa_y(t_i)$, which is (55) for $\lambda_0=\lambda_2=0$.

APPENDIX G: DETERMINATION OF THE SOLUTION OF THE OPTIMAL δ-ROBUST POPULATION TRANSFER

In Sec. VII we showed that a resonant pulse $\Delta=0$ is the solution of the optimal δ-robust population transfer. The pulse shape is determined from the pendulum differential equation

$$-\ddot\theta\pm\lambda\cos\theta=0, \quad \text{(G1)}$$

where the $\pm$ sign is correlated with the sign of γ with the constraint

$$\int_0^T dt\,\sin\theta(t)\sin\gamma(t)=0. \quad \text{(G2)}$$

We notice that $\sin\gamma$ has to change its sign in order to satisfy the above constraint. We assume that it happens at a time t_1, which leads to (taking $\gamma=+\pi/2$ for $0\leqslant t<t_1$)

$$\int_0^{t_1} dt\,\sin\theta(t)-\int_{t_1}^{T} dt\,\sin\theta(t)=0. \quad \text{(G3)}$$

We show below that it happens when the trajectory reaches the south pole of the Bloch sphere, when the transfer becomes complete. We take initially $\gamma_i=\varphi_i=\pi/2$.

The propagator for a chosen positive Ω reads

$$U_1(t,0)=\begin{bmatrix}\cos(A/2) & -i\sin(A/2)\\ -i\sin(A/2) & \cos(A/2)\end{bmatrix},\quad A=\int_0^t\Omega(s)ds, \quad \text{(G4)}$$

where A is the pulse area (and $\dot A>0$). The solution $|\phi(t)\rangle=U(t,0)|\phi(0)\rangle$ can be written as

$$|\phi(t)\rangle=\begin{bmatrix}\cos(A/2)\\ -i\sin(A/2)\end{bmatrix}=\begin{bmatrix}e^{i\pi/4}\cos(\theta/2)\\ e^{-i\pi/4}\sin(\theta/2)\end{bmatrix}e^{-i\pi/4}, \quad \text{(G5)}$$

i.e., with $\gamma=\varphi=\pi/2$ and $\theta\equiv A$, until $t=t_1$. When $A>\pi$, for $t>t_1$, we have $\theta=2\pi-A$, i.e., $\dot\theta=-\dot A<0$, and the solution reads

$$|\phi(t)\rangle=\begin{bmatrix}-\cos(\theta/2)\\ -i\sin(\theta/2)\end{bmatrix}=\begin{bmatrix}e^{-i\pi/4}\cos(\theta/2)\\ e^{i\pi/4}\sin(\theta/2)\end{bmatrix}e^{-3i\pi/4}, \quad \text{(G6)}$$

i.e., with $\varphi=-\pi/2$ and $\gamma=3\pi/2$. The change of γ from $\pi/2$ to $3\pi/2$ (i.e., the change of sign of $\sin\gamma$) occurs thus when the trajectory just overcomes the south pole of the Bloch sphere. It also goes with a change of sign of φ, from $\pi/2$ to

$-\pi/2$, and a change of sign of $\dot{\theta}$, from positive to negative, until $\Omega = 0$ at time t_2, for which the solution reads [with $\theta_2 \equiv \theta(t_2) > \pi$]

$$|\phi(t_2)\rangle = \begin{bmatrix} -\cos(\theta_2/2) \\ -i\sin(\theta_2/2) \end{bmatrix}. \tag{G7}$$

When Ω becomes negative, we have the subsequent partial area $A' = -\int_{t_2}^{t} \Omega(s)ds$, i.e., $\dot{\theta} > 0$. This can be seen from the formula $\dot{\theta} = \Omega \sin\varphi$, with $\Omega < 0$ and $\varphi = -\pi/2$. For such negative Ω, the propagator reads

$$U_2(t,0) = \begin{bmatrix} \cos(A'/2) & i\sin(A'/2) \\ i\sin(A'/2) & \cos(A'/2) \end{bmatrix}, \tag{G8}$$

with

$$A' = -\int_{t_2}^{t} \Omega(s)ds = \theta(t) - \theta_2, \tag{G9}$$

and the solution reads

$$|\phi(t)\rangle = \begin{bmatrix} \cos(A'/2) & i\sin(A'/2) \\ i\sin(A'/2) & \cos(A'/2) \end{bmatrix} \begin{bmatrix} -\cos(\theta_2/2) \\ -i\sin(\theta_2/2) \end{bmatrix}, \tag{G10}$$

i.e., at the final time $t = T$,

$$|\phi(T)\rangle = \begin{bmatrix} -\cos[(A'_T + \theta_2)/2] \\ -i\sin[(A'_T + \theta_2)/2] \end{bmatrix}, \quad A'_T = A'(t = T). \tag{G11}$$

The transfer is complete when

$$A'_T + \theta_2 = \pi, \quad \text{i.e., } A_2 - A'_T = \pi. \tag{G12}$$

In summary, the pulse is decomposed as a first positive part featuring a monotonically increasing θ with $\varphi = \gamma = \pi/2$ until the π area and next a change of sign of φ to $-\pi/2$ with $\gamma = 3\pi/2$ and a monotonically decreasing θ until $\dot{\theta} = 0$, followed by a negative part with a monotonically increasing θ, with $\varphi = -\pi/2$ and $\gamma = 3\pi/2$.

The precise dynamics is given by Eqs. (83): Eq. (83a) corresponds to $\lambda_1 = 0$ at resonance and Eq. (83b) reduces to an equation involving only λ_2 (denoted by λ) and a constant γ,

$$\ddot{\theta} - \lambda \sin\gamma \cos\theta = 0, \tag{G13}$$

where $\sin\gamma = \pm 1$. The solution can be obtained as follows. We multiply both sides by $\dot{\theta}$ and integrate (where c_1 is a constant):

$$\tfrac{1}{2}\dot{\theta}^2 = \lambda \sin\gamma \sin\theta + c_1. \tag{G14}$$

We then obtain

$$\frac{d\theta}{\sqrt{2\lambda\sin\gamma\sin\theta + 2c_1}} = \pm dt, \tag{G15}$$

where the sign $+$ $(-)$ stands for $\dot{\theta} > 0$ $(\dot{\theta} < 0)$ and is correlated with the sign of $\sin\gamma$. This can be rewritten to make appear an elliptic integral using $u = \pi/2 - \theta$ such that $\sin\theta = \cos u = 1 - 2\sin^2(u/2)$ and $x = -u/2 = \theta/2 - \pi/4$,

$$\frac{2dx}{\sqrt{2\lambda\sin\gamma(1 - 2\sin^2 x) + 2c_1}} = \pm dt, \tag{G16}$$

i.e., if $c_1 + \lambda\sin\gamma > 0$,

$$\frac{dx}{\sqrt{1 - m\sin^2 x}} = \pm\omega dt, \tag{G17}$$

with

$$m = \frac{2\lambda\sin\gamma}{\lambda\sin\gamma + c_1}, \quad \omega = \sqrt{\frac{c_1 + \lambda\sin\gamma}{2}}. \tag{G18}$$

The integration gives

$$\int^{\nu} \frac{dx}{\sqrt{1 - m\sin^2 x}} = \pm\omega t + c_2, \quad \nu = \frac{\theta}{2} - \frac{\pi}{4}, \tag{G19}$$

i.e., in terms of the incomplete elliptic integral of the first kind defined as

$$F(\nu, m) = \int^{\nu} \frac{dx}{\sqrt{1 - m\sin^2 x}}, \tag{G20}$$

$$F(\theta_\pm/2 - \pi/4, m) = \pm\omega t + c_2, \tag{G21}$$

where θ_+ (θ_-) is associated with $\dot{\theta}_+ > 0$ $(\dot{\theta}_- < 0)$. Equation (G19) shows that $-\pi/4 \leqslant \nu \leqslant \pi/4$, imposing $m < 2$ on the full range of $\theta \in [0, \pi]$, and, from (G18), $c_1 > 0$. This gives, after inversion,

$$\theta_\pm(t) = 2\,\mathrm{am}(\pm\omega t + c_2, m) + \frac{\pi}{2}, \tag{G22}$$

with $\mathrm{am}(u, m)$ the Jacobi amplitude function, the inverse of the incomplete elliptic integral

$$F(\nu, m) = u \Longleftrightarrow \nu = \mathrm{am}(u, m). \tag{G23}$$

Otherwise, if $c_1 + \lambda\sin\gamma < 0$, the integral (G16) can be written in the form

$$\frac{dx}{\sqrt{-1 + m\sin^2 x}} = \pm\sqrt{-\frac{c_1 + \lambda\sin\gamma}{2}}dt, \tag{G24}$$

which, if additionally $c_1 - \lambda\sin\gamma > 0$, i.e.,

$$\lambda\sin\gamma < c_1 < -\lambda\sin\gamma, \quad \lambda\sin\gamma < 0, \tag{G25}$$

gives

$$\frac{dy}{\sqrt{1 - m_1\sin^2 y}} = \mp\omega_1 dt, \tag{G26}$$

with $y = x - \pi/2$ and

$$m_1 = \frac{2\lambda\sin\gamma}{\lambda\sin\gamma - c_1}, \quad \omega_1 = \sqrt{\frac{c_1 - \lambda\sin\gamma}{2}}. \tag{G27}$$

The integration gives

$$\int^{\nu} \frac{dy}{\sqrt{1 - m_1\sin^2 y}} = \pm\omega_1 t + c_2, \quad \nu = \frac{\theta}{2} - \frac{3\pi}{4}, \tag{G28}$$

i.e., in terms of the incomplete elliptic integral

$$F(\theta_\pm/2 - 3\pi/4, m_1) = \pm\omega_1 t + c_2, \tag{G29}$$

and after inversion

$$\theta_\pm(t) = 2\,\mathrm{am}(\pm\omega_1 t + c_2, m_1) + \frac{3\pi}{2}. \tag{G30}$$

The initial condition $\theta(t_i=0)\equiv\theta_i=0$, $\dot\theta(0)\equiv\dot\theta_i>0$, where we assume $\varphi_i=\gamma_i=\pi/2$, i.e.,

$$m=\frac{2\lambda}{\lambda+c_1},\quad \omega=\sqrt{\frac{\lambda+c_1}{2}},\tag{G31}$$

gives

$$F(\pi/4,m)=-c_2,\quad \dot\theta_i=\sqrt{2c_1}.\tag{G32}$$

We can use the pair of free parameters $\{\lambda,c_1\}$ or $\{m,\omega\}$. Equation (G31) gives $\{m,\omega\}$ from $\{\lambda,c_1\}$; conversely, the latter are obtained from the former by

$$\lambda=m\omega^2,\quad c_1=\omega^2(2-m).\tag{G33}$$

The angle $\theta(t)$ for time $t\in[0,t_1]$ is given by $\theta_+(t)$ of Eq. (G22), denoted by $\theta_0(t)$ and defined in (87), until $t=t_1$, for which $\theta=\pi$: $F(\pi/4,m)=\omega t_1+c_2$, i.e., Eq. (88). For time $t\in[t_1,t_2]$, where $\varphi=-\pi/2$ and $\gamma=3\pi/2$, i.e., $\sin\gamma=-1$, $\theta(t)$ is given by $\theta_-(t)$ of Eq. (G30), denoted by $\theta_1(t)$,

$$\theta_1(t)=2\,\mathrm{am}(-\omega' t+c_2',m')+\frac{3\pi}{2},\tag{G34}$$

with, from (G27),

$$m'=\frac{2\lambda}{\lambda+c_1'},\quad \omega'=\sqrt{\frac{c_1'+\lambda}{2}},\tag{G35}$$

where the constants c_1' and c_2' are given by the continuity $\theta_0(t_1)=\theta_1(t_1)=\pi$ and $\dot\theta_0(t_1)=-\dot\theta_1(t_1)$. The minus sign in the latter term is due to a change of sign of $\sin\varphi$ at t_1 if we assume the continuity of the field Ω [see (4a)]. This gives, for the derivatives $\dot\theta_0(t_1)=-\dot\theta_1(t_1)$, from (G15), $c_1'=c_1$, i.e.,

$$m'=\frac{2\lambda}{\lambda+c_1}=m>1,\quad \omega'=\sqrt{\frac{c_1+\lambda}{2}}=\omega,\tag{G36}$$

and for $\theta_0(t_1)=\theta_1(t_1)=\pi$,

$$\pi=2\,\mathrm{am}(-2F(\pi/4,m)+c_2',m)+\frac{3\pi}{2},\tag{G37}$$

i.e.,

$$c_2'=F(\pi/4,m),\tag{G38}$$

and finally

$$\theta_1(t)=2\,\mathrm{am}(-\omega t+F(\pi/4,m),m)+\frac{3\pi}{2}.\tag{G39}$$

The pulse becomes zero at t_2 for which $\dot\theta_1(t_2)=0$, i.e., when the squared root of (G28) (for $m_1\equiv m$) nullifies

$$\theta_1(t_2)=\frac{3\pi}{2}-2\arcsin(1/\sqrt{m}),\tag{G40}$$

which gives

$$t_2=[F(\pi/4,m)+F(\arcsin(1/\sqrt{m}),m)]/\omega.\tag{G41}$$

The subsequent negative part of the pulse (for time $t\in[t_2,T]$) is given by $\theta_+(t)$ of Eq. (G30), denoted by $\theta_2(t)$,

$$\theta_2(t)=2\,\mathrm{am}(\omega t+c_2'',m)+\frac{3\pi}{2},\tag{G42}$$

which ensures the continuity of the first derivatives $\dot\theta_1(t_2)=\dot\theta_2(t_2)$. The continuity $\theta_1(t_2)=\theta_2(t_2)$ gives

$$\begin{aligned}c_2''&=-F(\arcsin(1/\sqrt{m}),m)-\omega t_2\\&=-2F(\arcsin(1/\sqrt{m}),m)-F(\pi/4,m).\end{aligned}\tag{G43}$$

The final time T is such that

$$\theta_2(T)=2\,\mathrm{am}(\omega T+c_2'',m)+\frac{3\pi}{2}=\pi,\tag{G44}$$

i.e., Eq. (92). The constraint that has to be satisfied is Eq. (93). The above constraint does not depend on ω, but only on m as defined in (G31). We use ω to normalize time (i.e., time is in units of $1/\omega$), the $\dot\theta$'s (hence the amplitude of the Rabi frequency in units of ω), and the energy (in units of ω as well),

$$\mathcal{E}=\int_0^{t_1}dt\,\dot\theta_0^2+\int_{t_1}^{t_2}dt\,\dot\theta_1^2+\int_{t_2}^{T}dt\,\dot\theta_2^2,\tag{G45}$$

where $\dot\theta_0(t)$ is given by

$$\begin{aligned}\dot\theta_0(t)&=2\omega\frac{d}{du}\mathrm{am}(u,m)\quad\text{for } u=\omega t-F(\pi/4,m)\\&=2\omega\frac{1}{\frac{d}{dv}F(v,m)}\quad\text{for } v=\mathrm{am}(u,m)\\&=2\omega\sqrt{1-m\sin^2[\mathrm{am}(u,m)]}\\&=2\omega\sqrt{1-m\,\mathrm{sn}^2(u,m)}\\&=2\omega\sqrt{1-m\,\mathrm{sn}^2(\omega t-F(\pi/4,m),m)}\\&=2\omega\,\mathrm{dn}(\omega t-F(\pi/4,m),m),\end{aligned}\tag{G46}$$

with the Jacobi elliptic sine $\mathrm{sn}(u,m):=\sin[\mathrm{am}(u,m)]$ and the delta amplitude $\mathrm{dn}(u,m):=\sqrt{1-m\,\mathrm{sn}^2(u,m)}$; $\dot\theta_1(t)$ is given by

$$\begin{aligned}\dot\theta_1(t)&=-2\omega\sqrt{1-m\,\mathrm{sn}^2(\omega t-F(\pi/4,m),m)}\\&=-\dot\theta_0(t)\end{aligned}\tag{G47}$$

and $\dot\theta_2(t)$ by

$$\begin{aligned}\dot\theta_2(t)&=2\omega\,\mathrm{dn}(\omega t-F(\pi/4,m)-2F(\arcsin(1/\sqrt{m})),m)\\&=-2\omega\,\mathrm{dn}(\omega t-F(\pi/4,m),m)\\&=-\dot\theta_0(t).\end{aligned}\tag{G48}$$

Using (4a), we obtain, for the pulse amplitude,

$$\Omega(t)=\dot\theta_0(t)=2\omega\,\mathrm{dn}(\omega t-F(\pi/4,m),m).\tag{G49}$$

We obtain, for the energy (in units of ω), using the change of variable $s=\omega t$,

$$\mathcal{E}/\omega=4\int_0^{\omega T}ds\,\mathrm{dn}^2(s-F(\pi/4,m),m).\tag{G50}$$

[1] M. A. Nielsen and I. L. Chuang, *Quantum Computation and Quantum Information* (Cambridge University Press, Cambridge, 2000).
[2] N. V. Vitanov, A. A. Rangelov, B. W. Shore, and K. Bergmann, Stimulated Raman adiabatic passage in physics, chemistry, and beyond, Rev. Mod. Phys. **89**, 015006 (2017).
[3] K. Bergmann *et al.*, Roadmap on STIRAP applications, J. Phys. B **52**, 202001 (2019).
[4] S. Guérin, S. Thomas, and H. R. Jauslin, Optimization of population transfer by adiabatic passage, Phys. Rev. A **65**, 023409 (2002).
[5] J. Roland and N. J. Cerf, Quantum search by local adiabatic evolution, Phys. Rev. A **65**, 042308 (2002).
[6] D. Daems, S. Guérin, and N. Cerf, Quantum search by parallel eigenvalue adiabatic passage, Phys. Rev. A **78**, 042322 (2008).
[7] G. Dridi, S. Guérin, V. Hakobyan, H. R. Jauslin, and H. Eleuch, Ultrafast stimulated Raman parallel adiabatic passage by shaped pulses, Phys. Rev. A **80**, 043408 (2009).
[8] S. Dogra and G. S. Paraoanu, Perfect stimulated Raman adiabatic passage with imperfect finite-time pulses, J. Phys. B **55**, 174001 (2022).
[9] S. Wimperis, Broadband, narrowband, and passband composite pulses for use in advanced NMR experiments, J. Magn. Reson. A **109**, 221 (1994).
[10] H. K. Cummins, G. Llewellyn, and J. A. Jones, Tackling systematic errors in quantum logic gates with composite potations, Phys. Rev. A **67**, 042308 (2003).
[11] J. A. Jones, Designing short robust NOT gates for quantum computation, Phys. Rev. A **87**, 052317 (2013).
[12] G. T. Genov, D. Schraft, T. Halfmann, and N. V. Vitanov, Arbitrarily accurate pulse sequences for robust dynamical decoupling, Phys. Rev. Lett. **113**, 043001 (2014).
[13] B. T. Torosov and N. V. Vitanov, Arbitrarily accurate variable rotations on the Bloch sphere by composite pulse sequences, Phys. Rev. A **99**, 013402 (2019).
[14] H. L. Gevorgyan and N. V. Vitanov, Ultrahigh-fidelity composite rotational quantum gates, Phys. Rev. A **104**, 012609 (2021).
[15] M. Bando, T. Ichikawa, Y. Kondo, N. Nemoto, M. Nakahara, and Y. Shikano, Concatenated composite pulses applied to liquid-state nuclear magnetic resonance spectroscopy, Sci. Rep. **10**, 2126 (2020).
[16] B. T. Torosov, S. Guérin, and N. V. Vitanov, High-fidelity adiabatic passage by composite sequences of chirped pulses, Phys. Rev. Lett. **106**, 233001 (2011).
[17] E. Torrontegui, S. Ibàñez, S. Martínez-Garaot, M. Modugno, A. del Campo, D. Guéry-Odelin, A. Ruschhaupt, X. Chen, and J. G. Muga, Adv. At. Mol. Opt. Phys. **62**, 117 (2013).
[18] D. Guéry-Odelin, A. Ruschhaupt, A. Kiely, E. Torrontegui, S. Martínez-Garaot, and J. G. Muga, Shortcuts to adiabaticity: Concepts, methods, and applications, Rev. Mod. Phys. **91**, 045001 (2019).
[19] A. Ruschhaupt, X. Chen, D. Alonso, and J. G. Muga, New J. Phys. **14**, 093040 (2012).
[20] D. Daems, A. Ruschhaupt, D. Sugny, and S. Guérin, Robust quantum control by a single-shot shaped pulse, Phys. Rev. Lett. **111**, 050404 (2013).
[21] L. Van-Damme, D. Schraft, G. T. Genov, D. Sugny, T. Halfmann, and S. Guérin, Robust NOT gate by single-shot-shaped pulses, Phys. Rev. A **96**, 022309 (2017).
[22] X. Laforgue, X. Chen, and S. Guérin, Robust stimulated Raman exact passage using shaped pulses, Phys. Rev. A **100**, 023415 (2019).
[23] C. P. Koch, U. Boscain, T. Calarco, G. Dirr, S. Filipp, S. J. Glaser, R. Kosloff, S. Montangero, T. Schulte-Herbrüggen, D. Sugny, and F. K. Wilhelm, Quantum optimal control in quantum technologies. Strategic report on current status, visions and goals for research in Europe, EPJ Quantum Technol. **9**, 19 (2022).
[24] N. Khaneja, T. Reiss, C. Kehlet, T. Schulte-Herbrüggen, and S. J. Glaser, Design of NMR pulse sequences by gradient ascent algorithms, J. Magn. Reson. **172**, 296 (2005).
[25] L. S. Pontryagin, V. G. Boltyanskii, R. V. Gamkrelidze, and E. F. Mischenko, *The Mathematical Theory of Optimal Processes* (Wiley, New York, 1962).
[26] U. Boscain, G. Charlot, J.-P. Gauthier, S. Guérin, and H. R. Jauslin, Optimal control in laser-induced population transfer for two- and three-level quantum systems, J. Math. Phys. **43**, 2107 (2002).
[27] U. Boscain, M. Sigalotti, and D. Sugny, Introduction to the Pontryagin maximum principle for quantum optimal control, PRX Quantum **2**, 030203 (2021).
[28] L. Van Damme, Q. Ansel, S. J. Glaser, and D. Sugny, Robust optimal control of two-level quantum systems, Phys. Rev. A **95**, 063403 (2017).
[29] J. Zeng, C. H. Yang, A. S. Dzurak, and E. Barnes, Geometric formalism for constructing arbitrary single-qubit dynamically corrected gates, Phys. Rev. A **99**, 052321 (2019).
[30] G. Dridi, K. Liu, and S. Guérin, Optimal robust quantum control by inverse geometric optimization, Phys. Rev. Lett. **125**, 250403 (2020).
[31] D. Buterakos, S. Das Sarma, and E. Barnes, Geometrical formalism for dynamically corrected gates in multiqubit systems, PRX Quantum **2**, 010341 (2021).
[32] X. Laforgue, G. Dridi, and S. Guérin, Optimal robust stimulated Raman exact passage by inverse optimization, Phys. Rev. A **105**, 032807 (2022).
[33] X. Laforgue, G. Dridi, and S. Guérin, Optimal quantum control robust against pulse inhomogeneities: Analytic solutions, Phys. Rev. A **106**, 052608 (2022).
[34] M. Harutyunyan, F. Holweck, D. Sugny, and S. Guérin, Digital optimal robust control, Phys. Rev. Lett. **131**, 200801 (2023).
[35] J. Zhu, X. Laforgue, X. Chen, and S. Guérin, Robust quantum control by smooth quasi-square pulses, J. Phys. B **55**, 194001 (2022).
[36] H. R. Lewis and W. B. Riesenfeld, An exact quantum theory of the time dependent harmonic oscillator and of a charged particle in a time dependent electromagnetic field, J. Math. Phys. **10**, 1458 (1969).
[37] X. Chen and J. G. Muga, Engineering of fast population transfer in three-level systems, Phys. Rev. A **86**, 033405 (2012).
[38] E. Torrontegui, S. Martínez-Garaot, and J. G. Muga, Hamiltonian engineering via invariants and dynamical algebra, Phys. Rev. A **89**, 043408 (2014).
[39] U. Güngördü, Y. Wan, M. A. Fasihi, and M. Nakahara, Dynamical invariants for quantum control of four-level systems, Phys. Rev. A **86**, 062312 (2012).

[40] F. T. Hioe, N-level quantum systems with SU(2) dynamic symmetry, J. Opt. Soc. Am. B **4**, 1327 (1987).

[41] S. S. Ivanov and N. V. Vitanov, Composite two-qubit gates, Phys. Rev. A **92**, 022333 (2015).

[42] L.-M. Duan, M. D. Lukin, J. I. Cirac, and P. Zoller, Long-distance quantum communication with atomic ensembles and linear optics, Nature (London) **414**, 413 (2001).

[43] N. Sangouard, C. Simon, H. de Riedmatten, and N. Gisin, Quantum repeaters based on atomic ensembles and linear optics, Rev. Mod. Phys. **83**, 33 (2011).

[44] H. L. Gevorgyan and N. V. Vitanov, Deterministic generation of arbitrary ultrasmall excitation of quantum systems by composite pulse sequences, Phys. Rev. A **108**, 032614 (2023).

[45] X. Yang, X. Nie, T. Xin, D. Lu, and J. Li, Quantum control for time-dependent noise by inverse geometric optimization, arXiv:2205.02515.